Community Geothermal Modeling

of UC Berkeley Campus

Kecheng Chen (UCB)
Zhenxiang Su (UCB)
Kenichi Soga (UCB/LBNL)
Peter Nico (LBNL)
Patrick Dobson (LBNL)
Antoine Gautier (LBNL)
Jianjun Hu (LBNL)
Michael Wetter (LBNL)

July 30, 2021

1. Introduction

The objective of this work is to investigate the feasibility of upgrading the existing campus energy delivery system at UC Berkeley (UCB) to a fifth-generation district heating and cooling system (5GDHC) that includes geothermal heat/cold storage. A traditional district heating (DH) system consists of a centralized power station that feeds hot water or steam into pipes to distribute heat. The high temperature DH system suffers from significant heat losses and high installation costs (Sulzer et al., 2021). The 5GDHC on the other hand can reach high efficiency by operating at low temperature. The capacity to work in the heating or cooling mode independently of network temperature using bi-directional and decentralized energy flows is the key for 5GDHC (Buffa et al., 2019). Furthermore, the advantages of ground source heat pump (GSHP) compared to air source heat pump (ASHP) can be found in 5GDHC systems (Li et al., 2014). This is mainly because seasonally the ground has higher temperature in the heating mode (winter) and the lower temperature in the cooling mode (summer) with respect to air temperature, leading to higher seasonal performance of the system. For the above reasons, the current research focuses on examining the feasibility of the 5th generation DHC network for the UCB Campus energy system.

Because of the increasingly deteriorating state of the existing campus energy delivery system, UCB recognizes the need for a holistic and long-term study of the future of its campus energy delivery system. Under the "UCB Energy Delivery Options Analysis" project, UCB contracted an engineering consultancy company, Arup, to perform a study (Arup, 2015) with the intent to identify the best method of delivering heat and power to the UCB campus in the long term. By considering factors including general use and occupancy profile, proximity and load densities, the nodal approach has been considered towards effective energy delivery. It is proposed to divide the campus into five zones as shown in Figure 1.

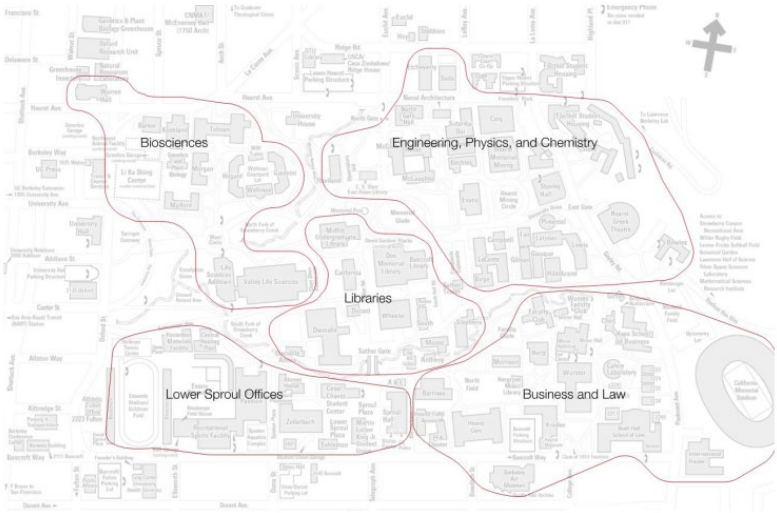

Figure 1 Campus zoning – nodal energy delivery approach

The energy delivery options considered by Arup (2015) are summarized in Table 1. After qualitative and quantitative analysis, Arup concluded that the Nodal heat recovery (NHR) option is an attractive strategy despite compounding uncertainty in future conditions. The NHR option supplies nodal chilled water and heating hot water using heat recovery chillers, gas-fired boiler (carbon capture and storage) /electric boiler/heat pump and electric chillers combined with hot and chilled water thermal energy

storage, battery storage, and distributed solar PV.

Table 1 Core energy delivery options

Option	Abbreviation	Generation System	Distribution
0	BL	Overhaul and continued operation of the existing system (Centralized gas-fired cogeneration)	Steam
1	NHR	Nodal heat recovery chillers, electric chillers, and gas-fired boilers	Chilled water (CHW) and heating hot water[23] (HHW)
2	CCG	Centralized cogeneration with combustion turbines	HHW and power
3	NHC	Nodal electric chillers and gas-fired boilers	CHW and HHW
4	NCG	Nodal cogeneration with combustion turbines	HHW and power
5	NCG-F	Nodal cogeneration with fuel cells	HHW and power
6	CGB	Centralized gas-fired boilers	HHW
7	DGB	Fully distributed condensing boilers	No campus distribution
8	CEB	Centralized all electric boilers	HHW
9	DEB	Fully distributed all-electric boilers	No campus distribution
10	CEB-S	Centralized all-electric boilers	Steam
11	CHC	Centralized electric chillers and gas-fired boilers	HHW and CHW
12	CHR	Centralized heat recovery chillers, electric chillers, and gas-fired boilers	HHW and CHW

The energy delivery options identified in the report require new, repurposed, and co-developed plants to house the proposed cogeneration, heating, and cooling equipment. The sizes of these plants are determined by the electric base loads, peak heating loads, and peak cooling loads of the campus buildings. In the Arup report, the plant footprints of the five zones are derived from equipment sizes using the reasonable assumptions. For the NHR option, the plant sitting, and the distribution routing are shown in Figure 2.

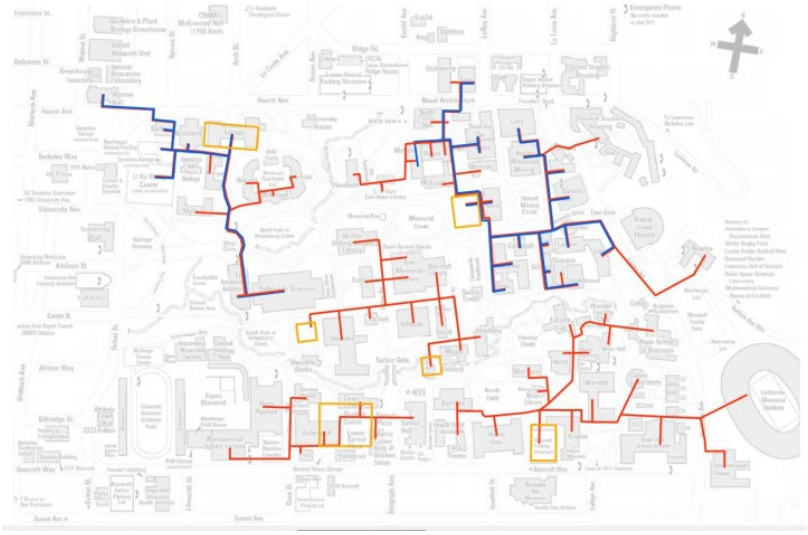

Figure 2 Plant siting and distribution routing basis – NHR option (Plant sites shown in yellow boxes; heating hot water (HHW) distribution routings shown in red lines; chilled water (CW) distribution routings shown in blue lines)

The work presented in this report is for the Bioscience node (the northwest corner of the campus) and the proposed plant is located at the old Tolman Hall site, which will house a new data hub building called the Gateway. The data for each building in the Bioscience node is shown in Table 2. Peak heating load is calculated from peak steam intensity and peak cooling load is calculated from total chiller capacity. The Commercial Prototype Building Models (CPBM), which were developed by researchers at the

Pacific Northwest National Laboratory (PNNL), are used to evaluate the energy demands of the UCB campus building types. The closest approximation is made by Arup based on model characteristics.

In this study, unscaled annual space heating/cooling and domestic hot water (DHW) load profiles are developed for each building using EnergyPlus simulations. This is described in Section 2. To ensure the actual demands are considered, the unscaled load profiles are scaled to match both the peak loads (the Syska Hennessey study for the existing buildings, from the UCOP study for the new buildings (Arup North America Ltd (2015)) and the electricity use intensities (EUIs) (measured or interpolated for the existing buildings, from the UCOP study for the new buildings (Arup North America Ltd (2015)) for each building. This will be described in Section 3.

An open space around Tolman Hall is selected for potential borehole installation. The size of ground source heat pump (GSHP) is designed based on ASHRAE's geothermal system design handbook to cover part of Bioscience node's heating and cooling demands. This is described in Section 4. Also, underground geothermal modeling is conducted using a high-performance computing (HPC) thermo-hydro coupling code developed by UCB researchers. This is described in Section 5.

Table 2 Building data of the Bioscience node

Building Name	Building Area (sqft)	Annual Electricity Use (kWh/yr)	Annual Steam Use (kBtu/yr)	Peak Heating Load (kBtu/h)	Peak Cooling Load (tons[1])
Barker Hall	86091	2816021	31229750	1557	200
Earl Warren Hall	69032	9034448	1559747	1784	200
Genetics & Plant Biology	26321	495637	-	521	66
Giannini Hall	68701	454653	5595752	1132	69
Hilgard Hall	77055	750964	10460320	1991	193
Koshland Hall	153700	7630965	48872025	2780	720
Li Ka Shing Center	220703	10551319	163657759	4990	1220
Morgan Hall	56637	975303	7945086	1171	85
Mulford Hall	93420	500760	13105035	1448	93
Northwest Animal Facility	52845	1281704	19169671	1195	132
University Hall	150887	1372861	2973104	3899	151
University House	18112	140096	1616931	371	13
Wellman Hall	43910	519010	5960842	908	44
Oxford Tract	1050000	3255000	14490000	11989	735
Tolman Hall (N) (Climate Science Building)	292500	4095000	24555375	9788	731

[1] 1 ton of cooling capacity is equal to 12000 BTUs per hour.

2. Commercial Prototype Building Model (CPBM) and EnergyPlus simulation

As part of DOE's support of ANSI/ASHRAE/IES Standard 90.1 and IECC, PNNL developed a suite of prototype buildings, which cover 75% of the commercial building floor area in the United States for new construction, including both commercial buildings and mid- to high-rise residential buildings, and across all U.S. climate zones. For the UCB project, Arup created a mapping table between its Commercial Prototype Building Models (CPBM) and the UCB campus building types by considering model characteristics (for example, high base load from hospitals, high DHW in hotels) corresponding to the ASHRAE Standard 90.1-2013. The mapping relationship is given in Table 3.

CPBM provides EnergyPlus model input files that can be used to conduct building simulation. EnergyPlus is a whole building energy simulation program that models both energy consumption—for heating, cooling, ventilation, lighting and plug and process loads—and water use in buildings. Based on the mapping relationship given in Table 3, the properties of CPBM including large hotel, hospital, secondary school, large office, and mid-rise apartment are checked and summarized in Table 4.

For a given set of heating, cooling, and service hot water (SHW) supply, the space heating, the space cooling and the DHW loads for each CPBM shown in Table 5 are computed. Cooling Coil Total Cooling Rate and Heating Coil Heating Rate are the rate of heat transfer taking place in the coil at the operating conditions for cooling and heating, respectively. These variables are determined by coil inlet and outlet air conditions and air mass flow rate through the coil. Water Heater Heating Energy is the heating energy supplied by a heater element or burner. The water heater objects are components for storing and heating water. Typical water heater applications are domestic hot water heating, low-temperature radiant space heating, and energy storage for solar hot water systems or waste heat recovery. Water Use Connections Plant Hot Water Energy is the plant loop energy consumed by the hot water used.

Table 3 Mapping between the CPBM and the UCB campus building type

	type	PNNL
0	Admin	Large Office
1	Athletic	Large Hotel
2	Data Center	Large Hotel
3	Auditorium	Large Office
4	Bioscience	Hospital
5	Chemistry	Hospital
6	Engineering	Hospital
7	Classroom	Secondary School
8	Residence	Mid-Rise Apartment
9	Mixed Use	Average of Engineering, Classroom, and Admin

Table 4 Summary of CPBM properties

CPBM	Mid-Rise apartment	Hospital	Large Hotel	Large office	Secondary school
HVAC System	All air system	All air system	All air system	All air system	All air system
Heating type	Gas furnace	Gas boiler	One gas-fired boiler	One gas-fired boiler	Gas furnaces inside packaged air conditioning units, Gas-fired boiler
Cooling type	Split system DX (1 per apt)	Two water cooled chillers	One air-cooled chiller	Water-source DX cooling coil with fluid cooler for datacenter in the basement and IT closets in other floors, Two water-cooled centrifugal chillers for the rest of the building	Packaged air conditioner, Air-cooled Chiller
SHW type	Individual residential water heater with storage tank	Main and central gas water heater with storage tank, Electric dishwasher booster water heater, Gas water heater for laundry with storage	Main and central gas water heater with storage tank, Electric dishwasher booster water heater, Gas water heater for laundry with storage	One main water heater with storage tank	Storage tank
Total floor area (ft^2)	33,700	241,410	122,132	498,600	210,900
Zone types	Apartment, Office, Corridor	Emergency Room, Office, Lobby, Nurse Station, Operating Room, Patient Room, Physical Therapy, Lab, Radiology, Dining, Kitchen, and Corridors	Basement, Retails, Lobby, Cafe, Laundry, Storage and Mechanical rooms, Guest rooms, Corridor, Banquet room, Dining, and Kitchen	Perimeter zones, Core zone, IT closet zone, Basement, Data center	Classrooms, Double loaded corridors, administrative areas, Gymnasium, auxiliary gym, auditorium, kitchen, and cafeteria

Table 5 Selection of output variables for each CPBM

CPBM	Mid-Rise apartment	Hospital	Large Hotel	Large office	Secondary school
Space heating	Heating Coil Heating Rate [W]	Heating Coil Heating Rate [W]	Heating Coil Heating Rate [W]	Heating Coil Heating Rate [W]	Heating Coil Heating Rate [W]
Space cooling	Cooling Coil Total Cooling Rate [W]	Cooling Coil Total Cooling Rate [W]	Cooling Coil Total Cooling Rate [W]	Cooling Coil Total Cooling Rate [W]	Cooling Coil Total Cooling Rate [W]
DHW	WATER HEATER:Water Heater Heating Energy [J]	Water Use Connections Plant Hot Water Energy [J]	Water Use Connections Plant Hot Water Energy [J]	Water Use Connections Plant Hot Water Energy [J]	Water Use Connections Plant Hot Water Energy [J]

To approximate the weather condition of the UCB site, the weather data of San Francisco is used (best approximation with weather data available in EnergyPlus weather format). This weather data is extracted from Typical Meteorological Year 2 (TMY2), which are the data sets of typical hourly values of solar radiation and meteorological elements for a 1-year period. TMY2 uses comprehensive methods that attempt to produce a synthetic year to represent the temperature, solar radiation, and other variables within the period of record, and more closely match the long-term average climatic conditions (Marion (1995)). Figure 3 shows the dry and wet bulb temperature changes of San Francisco in 2018. The space heating, space cooling and DHW loads per area for each CPBM are then calculated, as shown in Figure 4. From the load profiles, it can be found that the DHW load does not vary much through the year for all building types. This is because the hot water load is a base load that would be expected to be relatively

constant throughout the year. On the other hand, the space heating and space cooling profiles show seasonal effects.

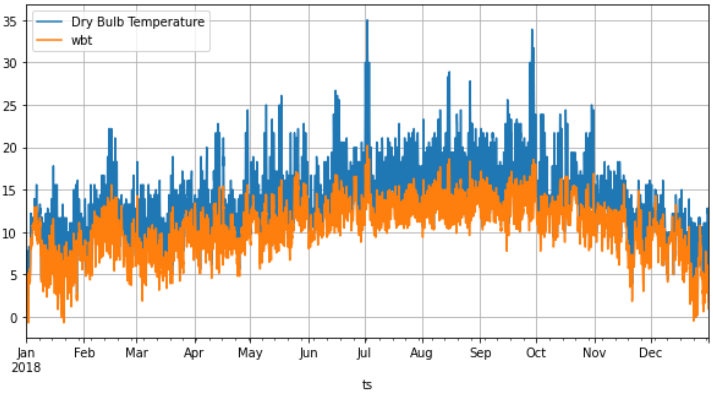

Figure 3 Dry and wet bulb temperature of San Francisco in degree Celsius

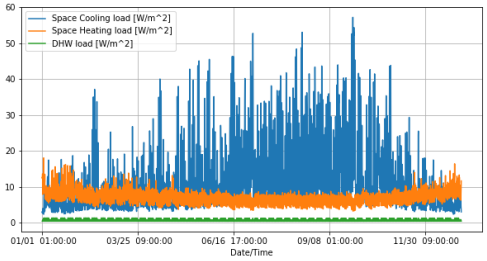

(a) Hospital

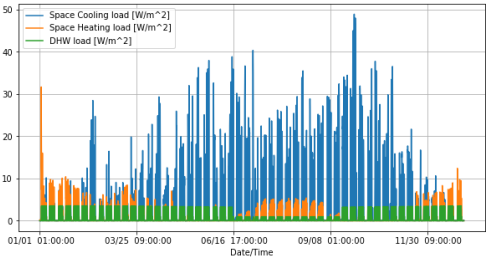

(b) Secondary school

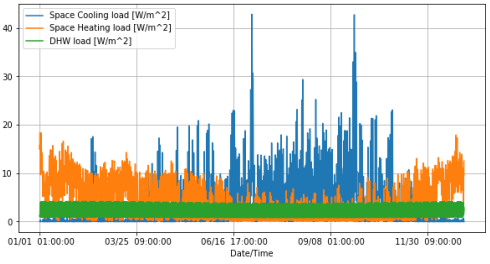

(c) Large hotel

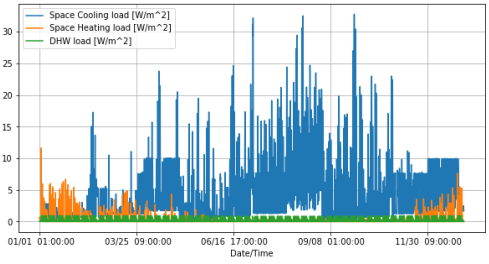

(d) Large office

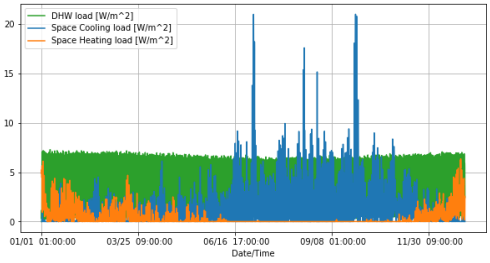

(e) Mid-rise apartment

Figure 4 Loads per area

The summation of the load profiles for the UCB campus building types and areas is conducted to generate the overall unscaled load profiles for the Bioscience node. This unscaled overall load profiles are shown in Figure 5. The heating load is the summation of the space heating and the DHW loads, whereas the cooling load is the space cooling load. These heating and cooling profiles give the reasonable

overall trends through the year for the Bioscience node based on the approximation made for each individual building. However, to evaluate the actual heating and cooling loads, these profiles need to be scaled to match the metered annual energy consumption and peak load data. This matching is conducted in the next section.

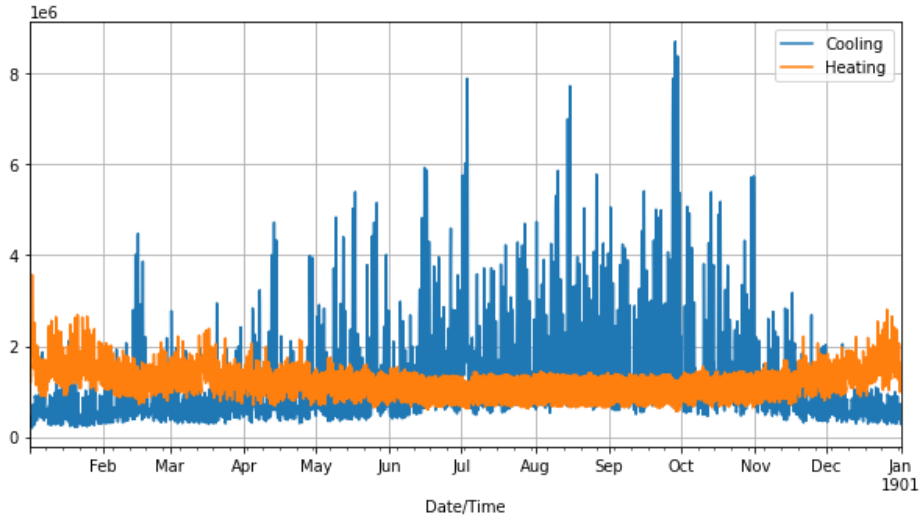

Figure 5 Overall unscaled load profiles [W] for the Bioscience node

3. Load Profiles Scaling

To generate the data for scaling, the constants and conversions proposed by Arup are used and they are listed in Table 6. Peak heating load is the peak of the summation of the space heating and the DHW loads, and peak cooling load is the peak of the space cooling load. Two load cases are proposed in this study. Load case 1 considers the straightforward profile scaling based on the Bioscience node's peak load and annual load. Load case 2 considers profile scaling based on each individual building's peak load and annual load, where the Bioscience node load profile would be the summation of each building's load profile.

Table 6 Constants and conversions

Parameter	Value	Unit	Source
Existing building-level steam loss	1.500000e-01	%	Assumption to convert from steam usage to heat...
Enthalpy	9.700000e+02	Btu/lb	NaN
Btu/kBtu	1.000000e+03	Btu/kBtu	Constant
Gas efficiency	8.000000e-01	%	Assumption
Btu per W	3.412000e+00	Btu/W	Constant
Btu per therm	1.000000e+05	Btu/therm	Constant
Absorption chiller efficiency	4.000000e-01	COP	Assumption based on average chiller age and di...
Existing electric chiller efficiency	1.250000e+00	kW/ton	Assumption based on average chiller age and di...
New electric chiller efficiency	5.000000e-01	kW/ton	Assumption based on average chiller age and di...
Building heating system efficiency	9.500000e-01	%	Assumption to convert from steam usage to heat...
Btuh per ton	1.200000e+04	Btuh/ton	Constant
J/Btu	1.055060e+03	NaN	NaN
kW/ton	3.516850e+00	NaN	NaN
kW/(kBtu/h)	2.930722e-01	NaN	NaN
J/kWh	3.600000e+06	NaN	NaN
m2/sqft	9.290300e-02	NaN	NaN

For Load case 1, the peak heating/cooling load for the Bioscience node is calculated by adding peak heating/cooling for each individual building in the node together and multiplying the node load diversity coefficient. As the annual energy consumption data are counted based on the steam use and electricity use separately, building heating system efficiency is used to convert the steam use to the annual heating energy and the average chiller coefficient of performance (COP) for the Bioscience node is used to convert the electricity usage to the annual cooling energy. As the chiller COP changes with respect to the ambient wet bulb temperature, more reasonable seasonal COP is calculated and used for conversion.

To scale the unscaled load profiles with respect to the peak load and annual energy, the following optimization function is formed.

$$\min_{k>0,b} \left\| \frac{Sum(k * L_{unscaled} + b) - E_{annual}}{E_{annual}} \right\|_2^2 + \left\| \frac{Max(k * L_{unscaled} + b) - P}{P} \right\|_2^2$$

where $L_{unscaled}$ is the unscaled heating or cooling load profile for the Bioscience node, E_{annual} is the annual heating or cooling energy consumption, and P is the peak heating or cooling load.

Python scipy package is used to find the optimization solution for solving this unconstrained multivariate scalar minimization function. The resulting scaled profiles are shown in Figure 6. After

checking, the annual energy consumption and peak load calculated from scaled load profiles are well matched with the metered data.

The Load Duration Curve (LDC) is an easy way of visualizing how consistently the Bioscience node is using the energy, and this is shown in Figure 7. The curve is the ordered load profile from the peak to the base. The horizontal axis represents the relative occupancy rate for the 1-year period. The cooling part of the node consumes energy less consistently than the heating part of the node. This is because the cooling load is relatively high due to the high internal gains through the summer. The corresponding load data statistics analysis is presented in Table 7.

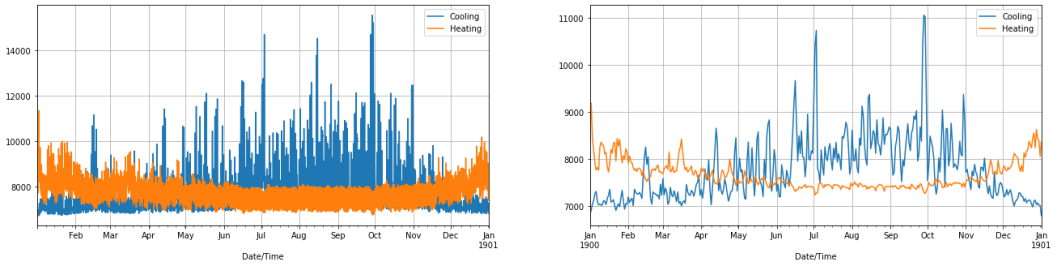

(a) Hourly sampling **(b) Daily sampling**

Figure 6 Overall scaled load profiles [kW] for the Bioscience node

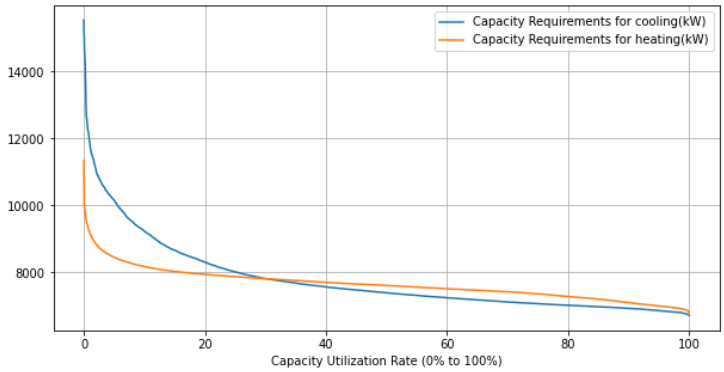

Figure 7 Load duration curve through the year

Table 7 Statistics of load Case 1 data [kW]

	Cooling	Heating
count	8760.000000	8760.000000
mean	7774.284835	7653.700033
std	1093.675191	454.445847
min	6715.631650	6741.506657
25%	7070.246206	7364.468016
50%	7393.533707	7612.389764
75%	8020.720815	7879.383653
max	15539.934468	11340.255047

For Load case 2, it is found that there are some individual buildings in the Bioscience node that do not have data or have highly data mismatch, and these errors are not considered in Load case 1. The ratios between the hourly average steam/electricity use and the hourly peak steam/electricity use were then checked. It was noted that buildings including Barker Hall, Koshland Hall, Li Ka Shing Center, Mulford Hall and Northwest Animal Facility have a steam use mismatch. The Genetics and Plant Biology building is missing its annual heating load data. In Arup's work, the annual load data were measured by UCB, and the peak load data were estimated from the existing facilities in each building. This data mismatch can happen because these two datasets are provided by different groups.

To have better load profiles, the profiles for the buildings with matched data are scaled based on both the Arup and UCB datasets, whereas those for the buildings with mismatched data are scaled based on the peak load, which represents the maximum capacity. After this re-scaling, the Genetics and Plant Biology building's annual heating loads are checked and compared with the loads of the other buildings. Results show that the data of this building matched well with others, as shown by the red points in Figure 8. The final scaled load profile of the Bioscience node is shown in Figure 9 and the corresponding load data statistics analysis is shown in Table 8.

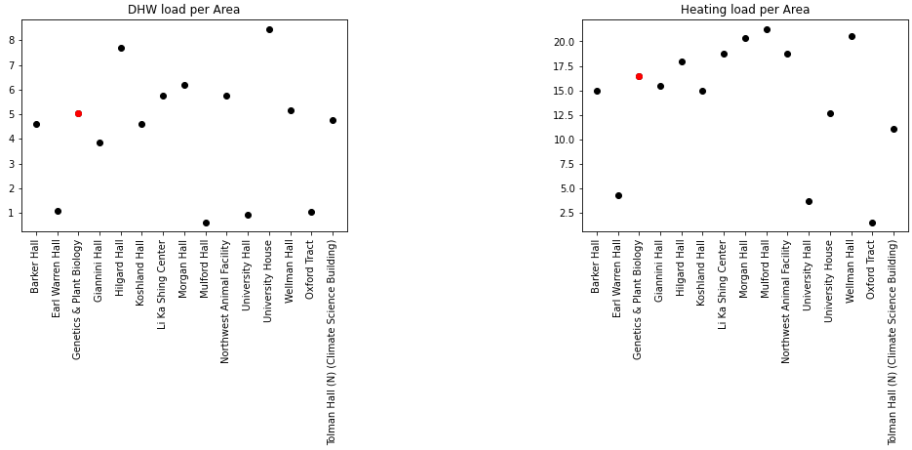

(a) DHW load **(b) Heating load**

Figure 8 Annual load per area [kW]

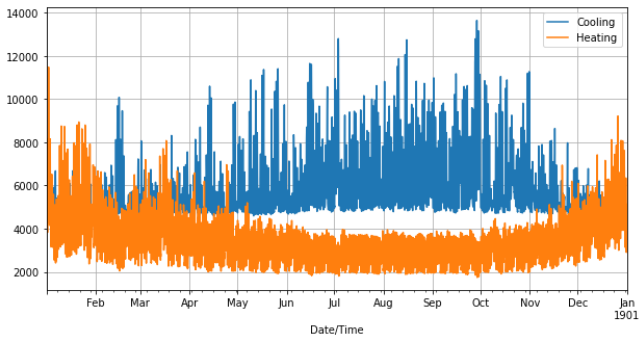

Figure 9 Summation of each individual building's scaled load profile [kW]

Table 8 Statistics of load Case 2 data [kW]

	Heating	Cooling
count	8760.000000	8760.000000
mean	3364.627777	5704.739595
std	973.077936	1429.589564
min	1743.566728	4416.054520
25%	2643.518394	4810.152693
50%	3311.758165	5083.009501
75%	3808.982341	5933.874691
max	11481.562662	13641.755282

4. GSHP Design

4.1 GSHP location

UCB is developing a campus geographic information system (GIS) to capture and analyze its spatial and geographic data of its facilities and services. The load of each building in the UCB campus is visualized in Figure 10, including peak heating, peak cooling, annual electricity use intensity, and annual steam use intensity. For the buildings in the Bioscience node, it is found that some buildings with high peak heating load also have high peak cooling load. These buildings are located sparsely, and they include Barker Hall, Li Ka Shing Center, Edwards Stadium, Tolman Hall, and Koshland Hall. With respect to annual energy consumption, these five buildings occupy 53% of the annual electricity use and 66% of the annual steam use of the Bioscience node.

(a) Peak heating (kBtu/hr)

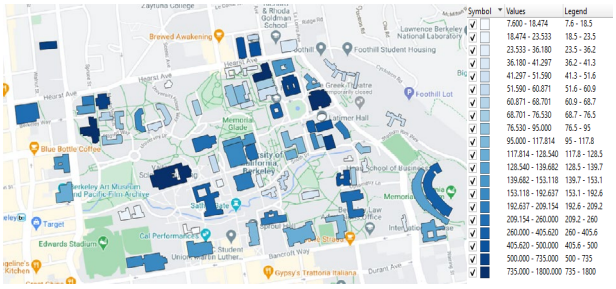

(b) Peak cooling (tons)

(c) Annual electricity use intensity (kWh/sqft*yr)

(d) Annual steam use intensity (kBtu/sqft*yr)

Figure 10 Peak load and annual EUI distribution map

Figure 11(a) and (b) show the utility pipelines distribution and available empty area surrounding Tolman Hall. Arup recommends placing the plant at the new Gateway building. As borehole installation should avoid the distribution utility pipelines and the GSHP network should be connected easily to the plant, the space east of University House is identified as one of the potential areas for GSHP installation, as shown in Figure 11(c), where the area is 200 m x 64 m.

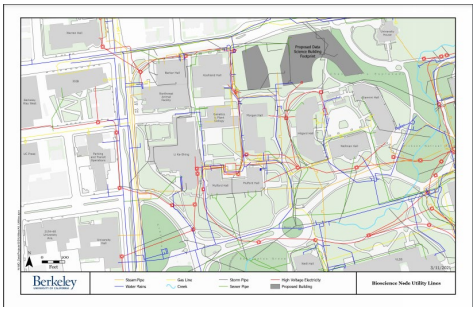

(a) Utility pipelines

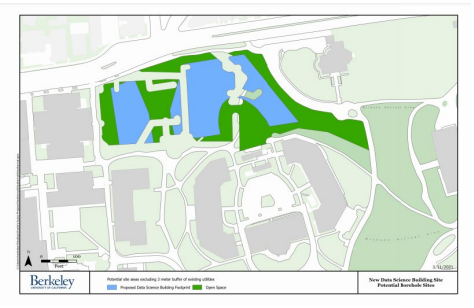

(b) Available empty area surrounding the Tolman Hall

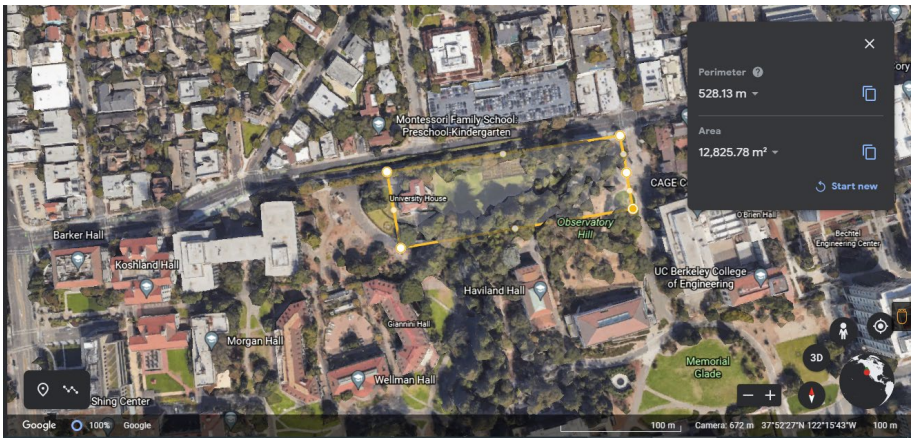

(c) Potential area for GSHP installation

Figure 11 Information for GSHP installation area selection

4.2 Borehole design

An equation for estimating ground heat exchanger bore length is referenced from ASHRAE's geothermal heating and cooling handbook.

$$L_c = \frac{q_a R_{ga} + q_{cond}\left(R_b + PLF_m R_{gm} + F_{sc} R_{gst}\right)}{t_g - \frac{ELT + LLT}{2} + t_p}$$

$$L_h = \frac{q_a R_{ga} + q_{evap}\left(R_b + PLF_m R_{gm} + F_{sc} R_{gst}\right)}{t_g - \frac{ELT + LLT}{2} + t_p}$$

where variables can be referenced as the following.

F_{sc} = short-circuit heat loss factor between supply and return tubes in bore (see Figure 3.7)
L_c = required bore length for cooling, ft (m)
L_h = required bore length for heating, ft (m)
PLF_m = part-load factor during design month
q_a = net annual average heat transfer to the ground, Btu/h (W)
R_{ga} = effective thermal resistance of the ground—annual pulse, h·ft·°F/Btu (m·K/W)
R_{gst} = effective thermal resistance of the ground—short-term pulse, h·ft·°F/Btu (m·K/W)
R_{gm} = effective thermal resistance of the ground—monthly pulse, h·ft·°F/Btu (m·K/W)
R_b = thermal resistance of bore, h·ft·°F/Btu (m·K/W)
t_g = undisturbed ground temperature, °F (°C)
t_p = long-term ground temperature penalty caused by ground heat transfer imbalances, °F (°C)
ELT = heat pump entering liquid temperature, °F (°C)
LLT = heat pump leaving liquid temperature, °F (°C)

Assumptions for the design is shown as the following.

- DR 11 HDPE pipe
- Vertical U-tube = 1.0 in. nominal,
- Borehole diameter = 5 in.
- Static water table at 10 ft below surface.
- Heat pulse analysis is done based on twenty-year (7300 day), one month (30 day), and six-hour (0.25 day).

Borehole design calculation considers the balance of the heat to the ground. Parameters used in the design are shown in Table 9. The Heating/cooling COP are determined referring to Carrier's fixed-speed water-sourced screw heat pump 30XWHP, which has a nominal cooling capacity of 1760 kW and a nominal heating capacity of 2030 kW, which is shown in Figure 12. According to AHRI Ground Source Closed-Loop Heat Pumps Standard, the test condition shall use antifreeze fluid, and the fluid temperature entering the heat exchanger in the cooling mode shall be 25°C and that in the heating mode shall be 0°C. However, this standard reflects operating condition of a cold climate residential closed-loop system and is not appropriate for typical commercial applications. In other words, low ground loop liquid temperature would cause a high compressor lift. If this lift is higher than the ASHP, then it is not possible to have benefits by using GSHP. Furthermore, by using antifreeze, both cooling and heating COP would be impacted as the characteristic of the fluid changes. In this study, the final entering evaporator temperature in the cooling mode is set to be 5 °C to 8 °C lower than the undisturbed ground temperature referring to the ASHRAE design handbook.

The Bioscience node is cooling-dominated and there is a need to balance the heat injection into the ground and the heat extraction from the ground. Hence, as shown in Figure 13, additional fluid cooler or cooling tower with an isolation heat exchanger is required with the ground loop to supply the cooling demand. However, if additional heating is needed, adding supplemental heating capacity in parallel or series with the ground loop is highly problematic because the possibility of high-temperature water entering the ground heat exchanger could result in failure of the HDPE tubing. Hence, energy recovery units and conventional air-side heat pump auxiliary heat, such as electrical resistance in the heat pump or hot-water distribution system, are considered to cover the rest of the heating loads.

The following three GSHP design options are proposed in this study. Option 0 considers using conventional GSHP system, which can provide heating or cooling. Option 1 and Option 2 both consider using a central GSHP system, which can provide simultaneous heating and cooling. Two different fluid cooler control methods are considered for these two options. In Option 1, the fluid cooler is always activated and covers specific portion of the heat rejection. In Option 2, the fluid cooler is activated when

the ground loop cannot meet the heat rejection requirements without assistance (Kavanaugh and Rafferty, 1998). Both Load case 1 and Load case 2 described in Section 3 are used for borehole design.

The borehole design details are given in Table 10. For both Load case 1 and Load case 2 with heat balance, the net base loads to the ground are similar and hence the design cases can be categorized to two clusters based on borehole numbers. In this way, two representative designs (800 numbers of 172.25 m borehole (Model 1) and 203 numbers of 180 m borehole (Model 2)) are examined in the underground thermal simulation section (Section 5).

Table 9 Parameters used for GSHP design

Variable	Description	Value
T_{HHW}	Heating hot water temperature	60 C
T_{CHW}	Chilled water temperature	3.3 C
$COP_{cooling}$	Heat pump cooling efficiency	5.5
$COP_{heating}$	Heat pump heating efficiency	3.5
t_a	Ground temperature	14.4 C
k_a	Ground conductivity	2.42 W/(mK)
a_a	Ground diffusivity	0.08 m^2/day
k_b	Bore fill conductivity	1.4 W/(mK)
ELT	Heat pump entering liquid temperature	25 C (cooling) / 8 C (heating)
LLT	Heat pump leaving liquid temperature	30 C (cooling) / 3 C (heating)
R_b	Average borehole resistance	0.15
F_{sc}	Short-circuiting heat loss factor	1.04

Table 10 Borehole design options and results

GSHP design option	Load case 1	Load case 2
Option 0	800 no. of 172.75m borehole	800 no. of 158.4m borehole
Option 1	203 no. of 180m borehole	309 no. of 180m
Option 2	123 no. of 200m borehole	280 no. of 200m borehole

Figure 12 Carrier's AquaForce - fixed-speed water-sourced screw heat pump 30XWHP

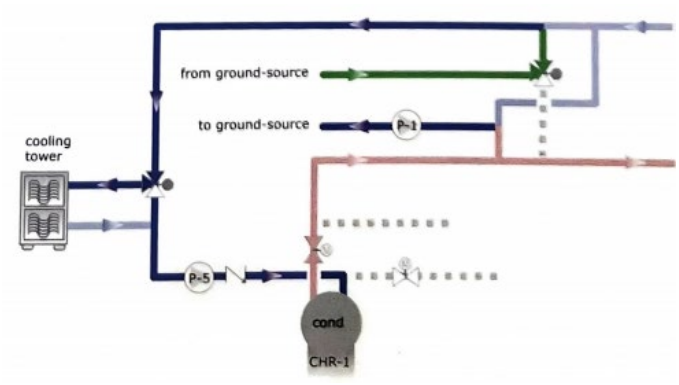

Figure 13 Supplemental heat rejection location downstream of ground-source

4.2.1 Option 0: Conventional GSHP system

For this conventional GSHP system option, the system cannot provide heating and cooling simultaneously. So rather than using the net load, the heating load and the cooling load should be considered separately in the design of GSHP. Also, because of the limitation of the installation area, GSHP is designed to cover one-third of the Bioscience node's demand, where the rest of the demand would be supplied by the auxiliary heater/cooler. The net loads to the ground for Load cases 1 and 2 are shown in Figure 14 and 15, respectively. For hourly net load in the Load case 1, the high loads around 1800 kW only appear several days in the summer cooling condition. For hourly net load in the Load case 2, the high loads around 2000 kW only appear several days in the winter heating condition. The 7-day average net load in both Load cases 1 and 2 shows that the net base load is close to 300 kW. The borehole design for GSHP is 800 boreholes each with a depth of 172.75m for Load case 1 and 800 boreholes each with a depth of 158.4m for Load case 2. The decrease in borehole depths for Load case 2 is because this option considers heating base load and cooling base load separately and the cooling base load, which dominates the design, is larger in Load case 1 than that in Load case 2, which decreases the design requirements for the length of the borefield heat exchange system of GSHP for Load case 2.

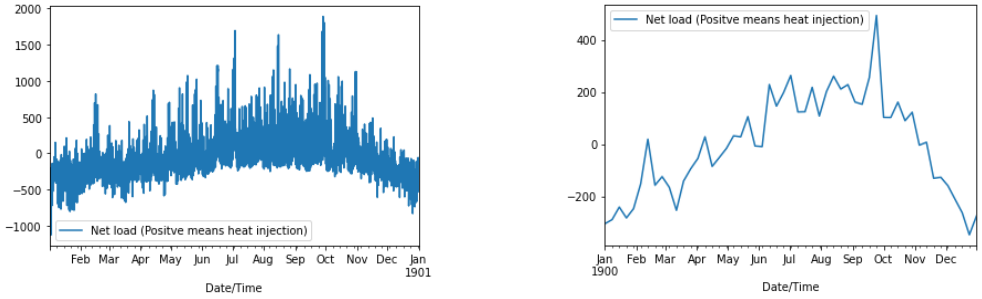

(a) Hourly **(b) 7-day average**

Figure 14 Net heat injection and heat extraction in the ground loop [kW] for Load case 1

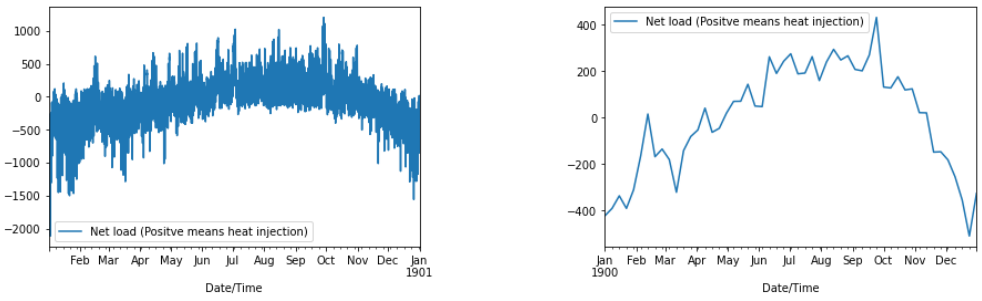

(a) Hourly **(b) 7-day average**

Figure 15 Net heat Injection and heat extraction in the ground Loop [kW] for Load case 2

4.2.2 Option 1 Central GSHP system 1

For simultaneous heating and cooling, a Multi-Chiller/Heater Cascading Plant developed by TRANE (see Figure 16) is used because of its high efficiency and energy sharing between heating and cooling zones. For this plant, the capacities of the heat pumps in the cooling mode are designed to meet the design cooling load, whereas the capacities of the heat pumps in the heating mode are designed to meet the design heating load.

For this Central GSHP system option, the fluid cooler is always activated and covers specific portion

of the heat rejection. GSHP is designed to cover the Bioscience node's demand. The net loads to the ground for Load cases 1 and 2 are shown in Figures 17 and 18, respectively. For hourly net load in the Load case 1, the high loads around 5000 kW only appear several days in the summer cooling condition. For hourly net load in the Load case 2, the high loads around 6000 kW only appear several days in the winter heating condition. The 7-day average net load in both Load cases 1 and 2 shows that the net base load is close to 600 kW.

In Option 1, for Load case 1, the design for the GSHP is 203 boreholes each with a depth of 180m, whereas, for Load case 2, the design for the GSHP is 309 boreholes each with a depth of 180m. The increase in borehole numbers for Load case 2 is because the difference between the heating base load and the cooling base load is much larger in Load case 2 than that in Load case 1, which increases the net load to the ground and further increases the design lengths of GSHP borefield heat exchange system.

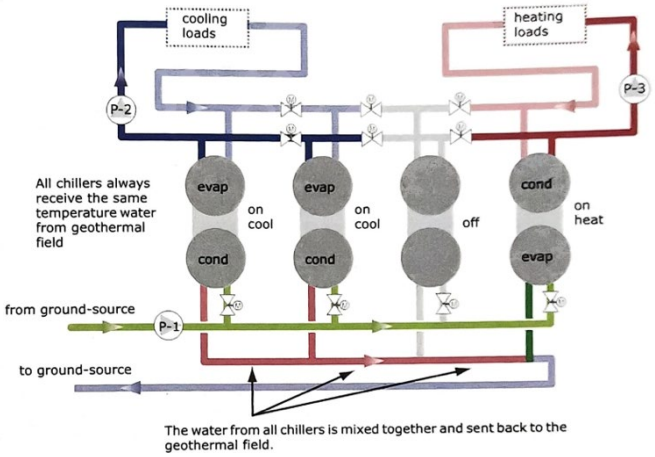

Figure 16 Water to water heat pump system coupled with a geothermal borefield

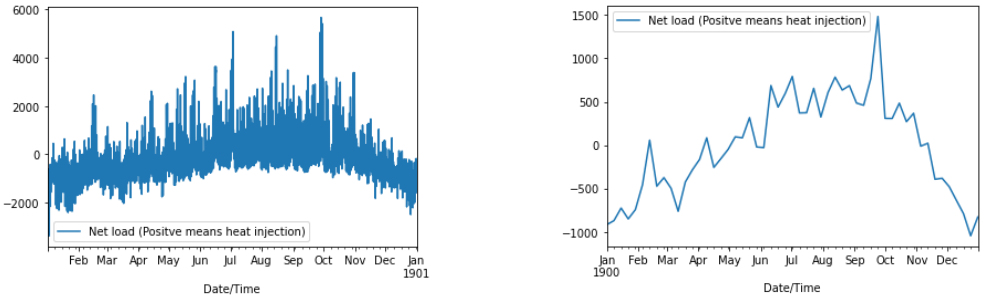

(a) Hourly **(b) 7-day average**

Figure 17 Net heat injection and heat extraction in the ground loop [kW] for Load case 1

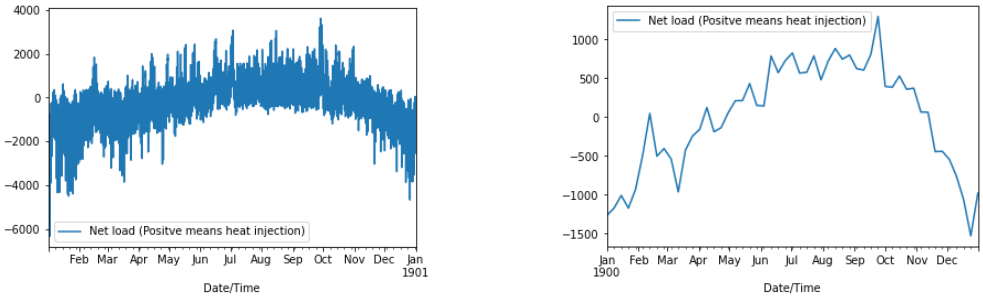

(a) Hourly **(b) 7-day average**

Figure 18 Net heat injection and heat extraction in the ground loop [kW] for Load case 2

4.2.2 Option 2: Central GSHP system 2

For this Central GSHP system option, the fluid cooler is activated when the ground loop cannot meet the heat rejection requirements without assistance. Because the chiller's control method can achieve a better overall efficiency, this option is well adopted in the industry. The design length is therefore highly dependent on the design heating load. According to ASHRAE's geothermal handbook, oversizing of heating and cooling systems is a common practice to offset uncertainties, but oversizing escalates borehole drilling costs. Considering the high capital cost for heat storage, GSHP is designed to cover the base load. As the high heating load conditions only appear for few days, the GSHP heating capacity is set to cover 96% of the heating conditions.

The hourly net loads to the ground for Load cases 1 and 2 are shown in Figure 19 and 20, respectively. For both Load cases 1 and 2, the net loads in the heating condition and the cooling condition are consistent, which is around 600 kW. For Load case 1, the design length for the GSHP is 123 boreholes each with a depth of 200m, whereas, for Load case 2, the design length for the GSHP is 280 boreholes each with a depth of 200m. The increase in the number of boreholes for Load case 2 can be explained by the same reason for Option 1.

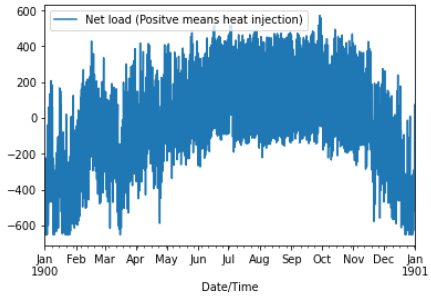

Figure 19 Hourly net heat injection and heat extraction in the ground loop [kW] for Load case 1

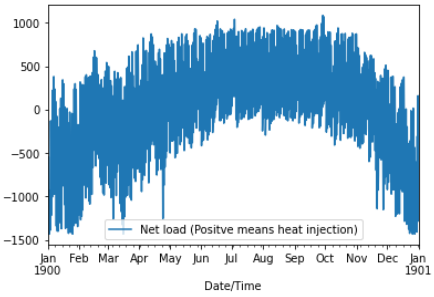

Figure 20 Hourly net heat injection and heat extraction in the ground loop [kW] for Load case 2

4.3 CO_2 and Electricity savings

The electricity savings made by replacing the air source heat pump (ASHP) in the NHR option with the ground source heat pump (GSHP) is estimated. The parameter used for the estimation is given in Table 11. The sub options of NHR are Option 1A, Option 1B and Option 1C. All three of these options use a nodal heat recovery chiller, but the difference is that for heating, Option 1A uses a gas boiler, Option 1B uses an electric boiler and Option 1C uses a heat pump. So, the Option 1C is investigated here. The heating efficiency for ASHP and GSHP can be derived referring to Arup's report and the Energy Star program separately. Since the heat pump is only used for heating in this option, electricity savings can be calculated from the annual heating energy for the Bioscience node.

Table 11 Parameters for savings calculation

Name	Source	Value
CO_2 intensity for electricity	PG&E	0.000262 tons/kWh (before 2045) / 0 tons/kWh (after 2045)
Heat recovery chiller heating offset for ASHP	Arup's report	40%
Hot water distribution loss	Arup's report	3%
Building heating system efficiency	Arup's report	95%
GSHP coefficient of performance (COP)	Energy Star	4
Annual cooling energy for Bioscience node	Arup's report	68101527.91 kWh
Annual heating energy for Bioscience node	Arup's report	67045120.06 kWh
Heating efficiency for ASHP	/	77.513 kWh/MMBtu
Heating efficiency for GSHP	/	61.49 kWh/MMBtu

The heating efficiency for ASHP and GSHP are calculated using the following functions.

$$Heating\ efficiency\ for\ ASHP/GSHP = \frac{1000}{EER \cdot (1 + heat\ recovery\ offset) \cdot (1 - loss) \cdot building\ heating\ system\ efficiency}$$

Based on the above, the annual electricity saving made by choosing the NHR option with GSHP rather than that with ASHP is 314835.84 kWh/year. If considering cooling recovery, the electricity saving can be further improved. California SB 100 sets a 100% clean, zero carbon, and renewable energy policy for California's electricity system by 2045. Based on the reduced use of the electricity, CO_2 savings before 2045 is calculated to be 82.5 tons/year.

4.4 Toward 5GDHC

Considering the system change from a central system to a distributed system (5GDHC) for heating and cooling, the number of boreholes needed can be calculated by assuming the adoption of 5GDHC can potentially provide 30% reduction for the overall load to GSHP. However, further work is needed to confirm this. For example, for 5GDHC (distributed HP), each building can reset the HW supply temperature when there is no DHW demand. If daily storage of DHW is considered at building level, the district plant can operate for only a few hours at 60℃ supply temperature until each building's DHW tanks are fully loaded, and then switch to the space heating mode. To determine the final plan for the GSHP, the whole heating and cooling network for the campus should be configured and the building-ground coupled simulation should be conducted to evaluate the optimized campus energy delivery method. This will be the next step of this study.

5. Underground thermal monitoring and modeling

5.1 Geological/Geotechnical information system of UCB campus

The project team is developing an underground geological and geotechnical information system database of the UCB campus. Geotechnical reports from past building projects have been checked for soil properties, exploratory boring log, surface elevation and water level. Previous boring locations are identified, as shown in Figure 21. The boring lithology data has been imported into Leapfrog Geothermal software for visualization and modeling, as shown in Figure 22. As the depths of the recorded boreholes are less than 30 m, a large 3D geologic map of the Hayward fault zone area by Phelps et al. (2008), which is available from USGS website, is also incorporated in the model to characterize the deeper geological condition. The project team is currently gathering near surface seismic data to provide more geologic information to a depth of 200 meters, which will be useful for the underground geothermal modeling of the UCB campus.

The project team has been collaborating with the UCB's facilities service department to install distributed fiber optic temperature sensors inside two geotechnical site investigation boreholes at O'Brien Hall with 30 feet depth and at Digital Hub Building with 70 feet depth (Figure 23(a) and (b)). The underground temperature profiles of these boreholes are measured every month to understand the seasonal variations. The thermal conductivity of core samples under fully dry and fully saturated conditions has been measured (Figure 23(c)) and the values are used for underground geothermal model simulations. An example of monthly thermal profile data is presented in Figure 24.

The project team will be installing a new 400 ft borehole in Fall, 2021 to conduct thermal response test as well as to install distributed fiber optics acoustic and temperature sensors and piezometers. The results of the installation, testing and monitoring will be reported in future reports. The data will be used to refine the underground geothermal model described in the next section.

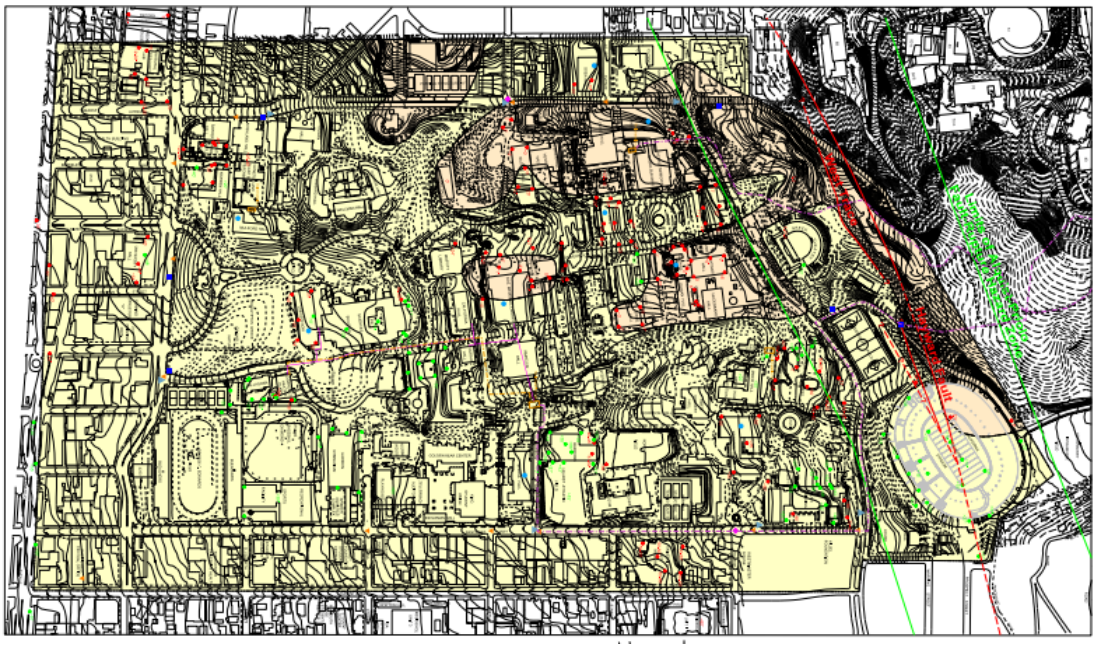

Figure 21 Campus topology and exploratory boring locations

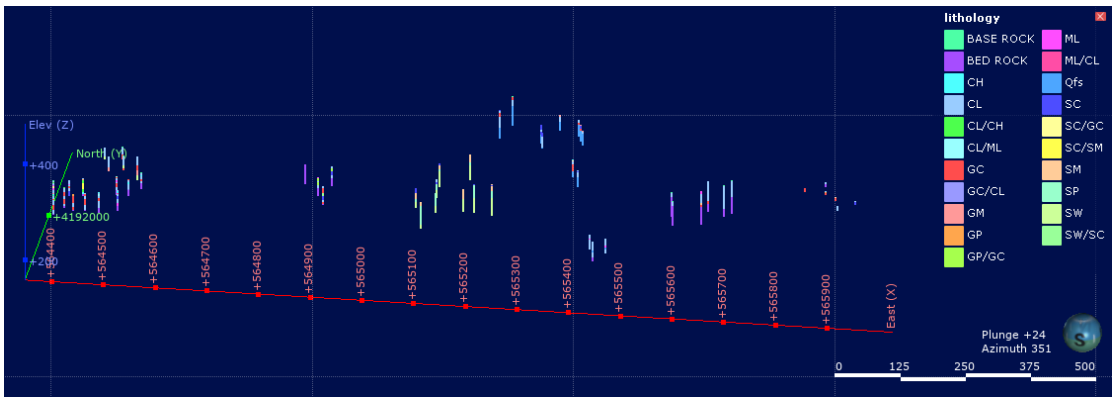

Figure 22 Boring data visualization

(a) Distributed fiber optic sensor installation

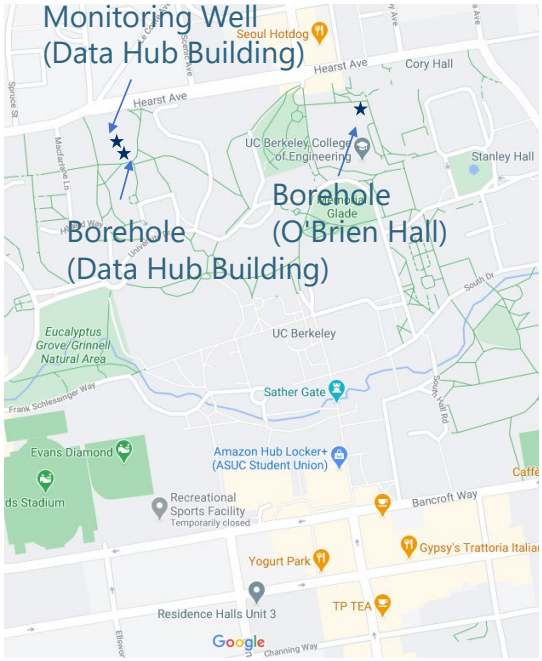

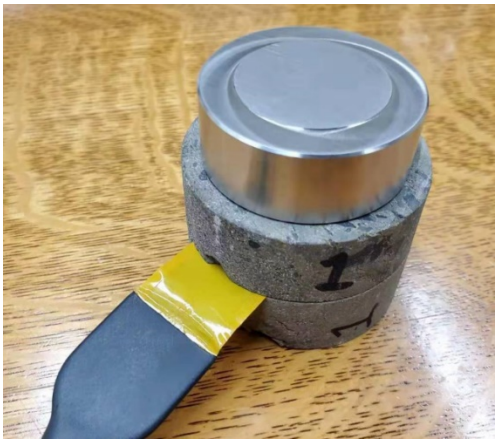

(b) Locations of distributed fiber optic sensor installation **(c) Thermal conductivity measurement**

Figure 23 Campus borehole monitoring

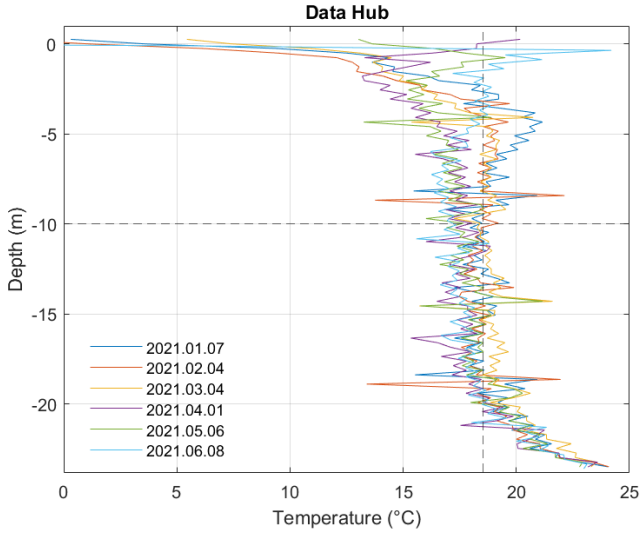

Figure 24 Monthly temperature profile monitoring (from Jan 2021 to June 2021)

5.2 UCB campus geothermal model

A UCB underground geothermal model has been developed in this preliminary study. The area of simulation includes the Berkeley campus and surrounding zone, as shown in Figure 25.

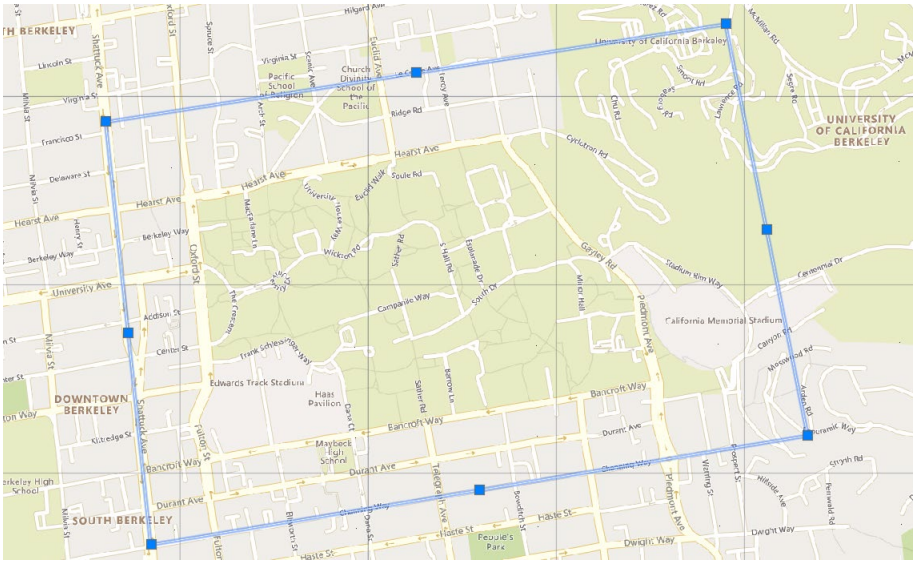

Figure 25 The area of simulation model

The model is constructed based on the 3D geologic map of the Hayward fault zone by Phelps et al. (2008). This map contains the locations and geometries of faults, ground surfaces and interfaces between geologic units. This map is imported into AutoCAD, and those parts within the simulation area are cut and converted into solid blocks, representing different geologic units as shown in Figure 26.

.

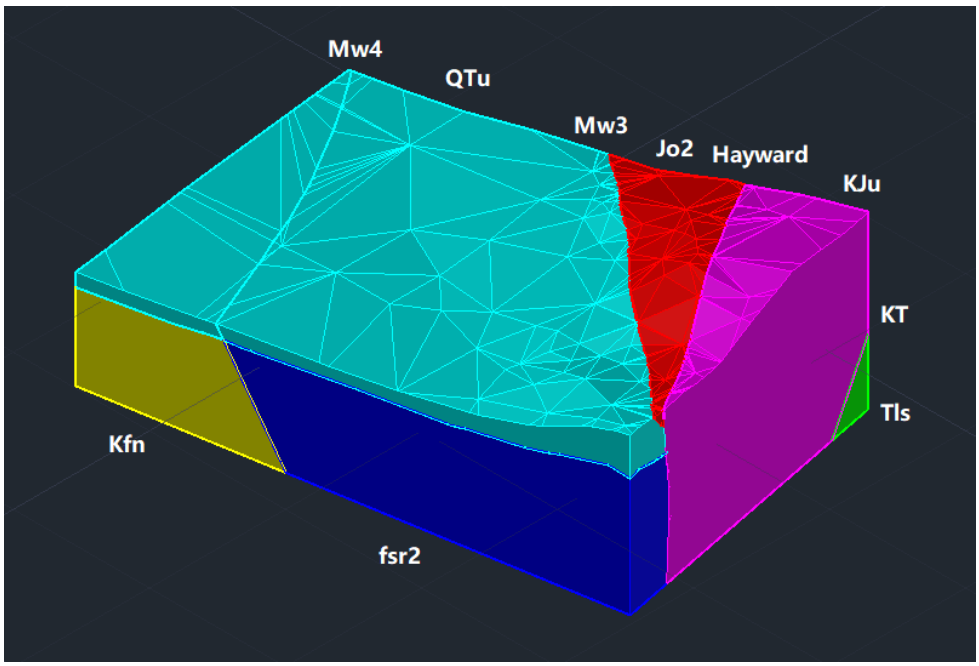

Figure 26 Blocks of geologic units

The labels of the faults and geologic units follows Phelps et al. (2008), and descriptions of these features are listed below.

Faults:

- Hayward: Hayward Fault
- Mw: Mesozoic faults
- KT: Cretaceous/Tertiary faults east of the Hayward Fault

Geologic units:

- QTu: Undivided Cenozoic sediments and sedimentary and volcanic rocks (Quaternary and Tertiary)
- fsr: Franciscan Complex mélange
- Kfn: Sandstone of the Novato Quarry terrane of Blake and others
- Jo: Undifferentiated Coast Range Ophiolite of the Great Valley Complex (Middle Jurassic)
- KJu: Undifferentiated Great Valley Complex rocks (Early Cretaceous and Late Jurassic)
- Tls: Undivided sedimentary and volcanic rocks (Miocene and Eocene)

The length and width of the model is approximately 1770 m and 1129 m, respectively. The model height varies from 310 m (southwest corner) to 574 m (northeast corner). This model is then imported into Gmsh (Geuzaine & Remacle, 2009) to generate the unstructured hexahedral mesh for finite element simulation. The boreholes are represented as line elements that are embedded in the mesh. The whole model is divided into three parts as shown in Figure 27. Part 1 is around the borehole area (~200 m x 64 m for Model 1; ~138 m x 48 m for Model 2), and the depth is 4m deeper than the bottom of the boreholes. The size of Part 2 is around (200 x 3) m x (64 x 3) m for Model 1, and around (138 x 3) m x (48 x 3) m for Model 2, both are around 50 m deeper than the bottom of the borehole. The rest is Part 3. The maximum sizes of hexahedral elements in these three parts are 2 m (Part 1), 8 m (Part 2) and 25 m (Part 3). There are around 1.9 million elements in total for Model 1, and around 1.3 million elements in total for Model 2, more than half of them are in Part 1.

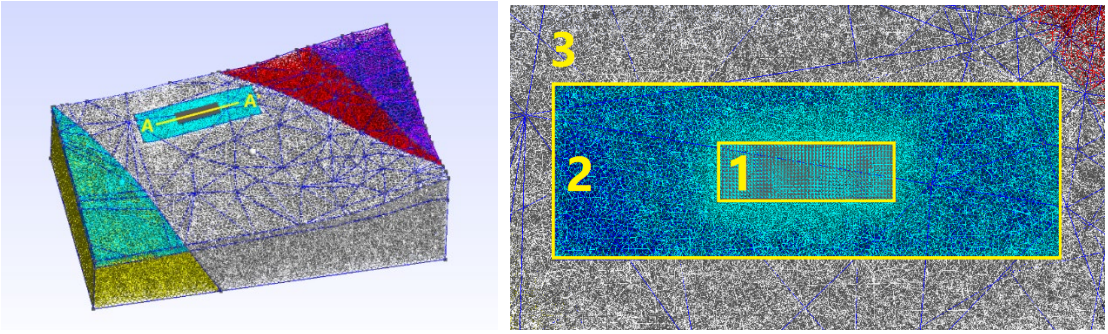

(a) Mesh generated using Gmsh; (b) Three parts with different mesh size

Figure 27 Mesh for ground model

5.3 Parameters and boundary conditions

As the available geological investigation data are from investigations conducted at much shallower range (within 30 m depth) compared with the target simulation region, the soil is assumed to be homogeneous with the same properties in this preliminary simulation. Future work will include data from a deeper borehole investigation planned in Fall 2021. The thermal capacity is taken to be 2.5e6 J/m^{3}K, which is a typical value for geo-materials. Soil conductivities are measured from several core samples and the values range from 1.8 to 2.5 W/mK. A value of 2 W/mK is used in this simulation. Two different permeability values, 1e-9 m/s and 1e-6 m/s are used to examine the effect of ground water flow on heat migration.

To account for the influence of seasonal changing atmosphere temperature, the ground surface is set to be temperature Dirichlet boundary. Previous building simulation uses weather data in San Francisco, as this is the closest TMY2 weather data available from EnergyPlus. As Oakland is closer to Berkeley compared with San Francisco and only atmospheric temperature data is needed, the boundary flux values are interpolated using the annual monthly average temperature measured at Oakland International Airport from the National Weather Service. The monthly average of these two datasets are plotted in Figure 28. Based on 30 years' weather data, TMY2 dataset selects 12 most typical months through empirical approach and concatenates them to form a typical year, while NOAA dataset gives the mean value over 30 years. The slightly difference between these two datasets may be due to variation of locations and data processing methods.

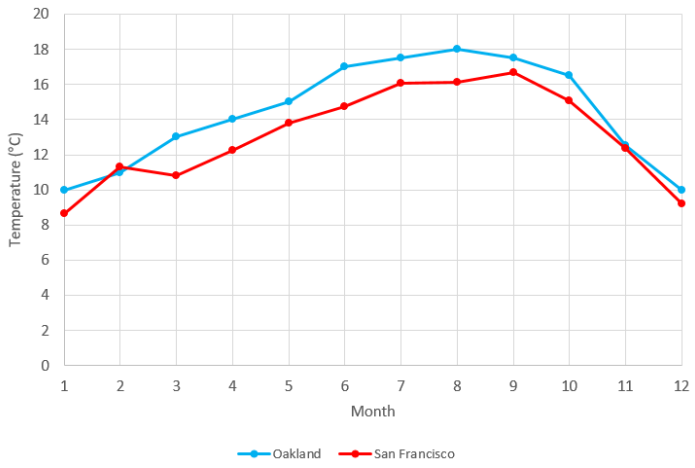

Figure 28 Annual monthly average temperature measured at Oakland International Airport (from NOAA) and San Francisco (From EnergyPlus)

The annual average temperature is around 14 °C, which happens in April. This value is used as the initial temperature of the ground surface. The initial underground temperature at other parts of the model is computed using the following equation.

$$T_0 = T_{top0} + depth \times T_{grad}$$

where T_{top0} is the ground initial temperature, T_{grad} is the temperature increment with depth and a typical value 0.03 K/m is used (ASHRAE, 2015).

The resulting initial temperature profile is shown in Figure 29. To keep the system static, the bottom surface is also set to be a temperature Dirichlet boundary and the values are also computed using the above formula. As the elevation of the ground surface varies, the initial temperatures are different even among those points that have the same z coordinates. The underground temperature monitoring currently conducted at the campus site will be used in the future to refine the temperature profile in the model.

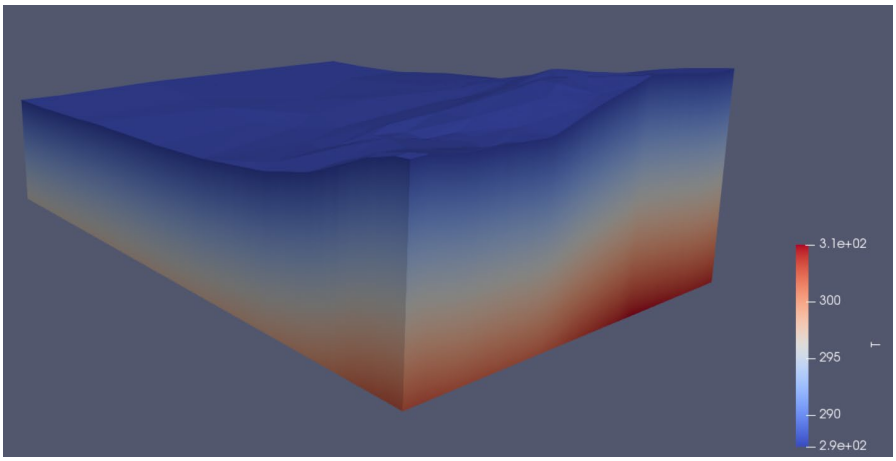

Figure 29 Initial temperature profile[2]

To exam the influence of the changing ground surface temperature along the depth, a one year simulation without the heat injecting/extraction from the model boreholes is conducted. The resulting temperature profile is shown in Figure 30. Results indicate that the influence of seasonal atmosphere temperature is up to 15m depth (see also the monitoring data presented in Figure 24), which is a reasonable value, but the appropriateness of the temperature boundary conditions will be examined in the future using the seasonal underground temperature monitoring data that the project team is currently collecting.

[2] Kelvin (K) = Celsius (°C) + 273.15

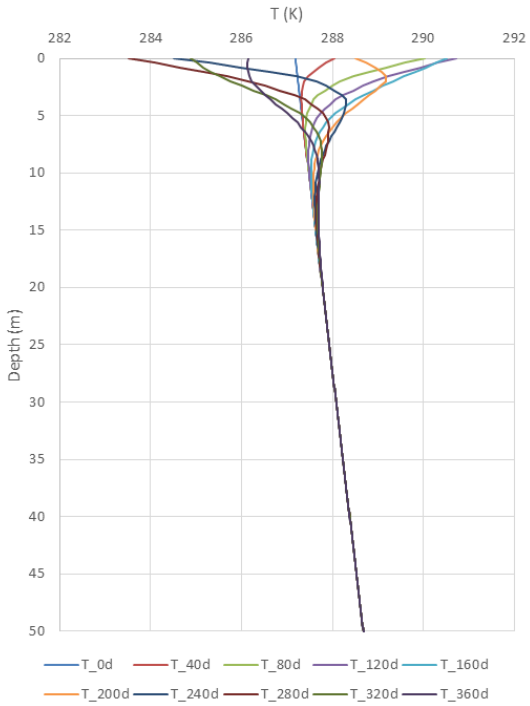

Figure 30 Influence of atmosphere temperature along depth

Previous site investigation data are available for the depths of groundwater table at selected locations inside the UCB campus. The values range between 0 and 11 m and the average value is around 5 m. With limited data available, the water table is assumed to be parallel with the ground surface and the depth is taken to be 5 m. The four side faces of the model are set as the pressure Dirichlet boundary, with the value increasing with depth. The initial groundwater pressure profile is shown in Figure 31.

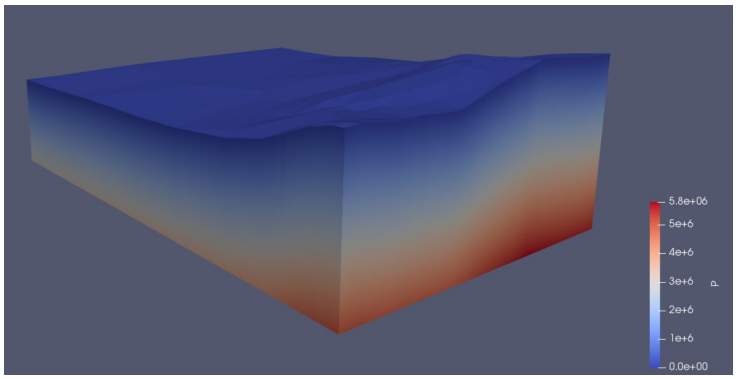

Figure 31 Initial ground water pressure profile

5.4 Borehole arrangement, loading profile and simulation results

The boreholes are modeled as line sources of heat flux, and the values are taken from the daily average power demand, which is presented earlier. The models 1 and 2 mentioned in Section 4 are used in the simulations. Their borehole arrangement and loading profiles are described below, followed by simulation results.

5.4.1 Model 1

5.4.1.1 Borehole arrangement and loading profile

In this model, there are 800 boreholes in total, each 172.75 m in length. This represents the conventional GSHP design (Option 0) described in Section 4. These boreholes are arranged in a 196 m by 60 m rectangular area in 16 rows. Each row has 50 boreholes. The spacing between adjacent boreholes is 4 m.

The daily power demands for one year are shown in Figure 32(a). The heating and cooling demands are approximately balanced; the average value throughout the year is small (-9.48e-6 kW). The amount of heat that is injected into and extracted from the ground are nearly the same in the one year period. To eliminate the effect of some extreme values, the moving averages with 19 days period are taken as shown in Figure 32(b). This demand plot is used as input loading for the simulations.

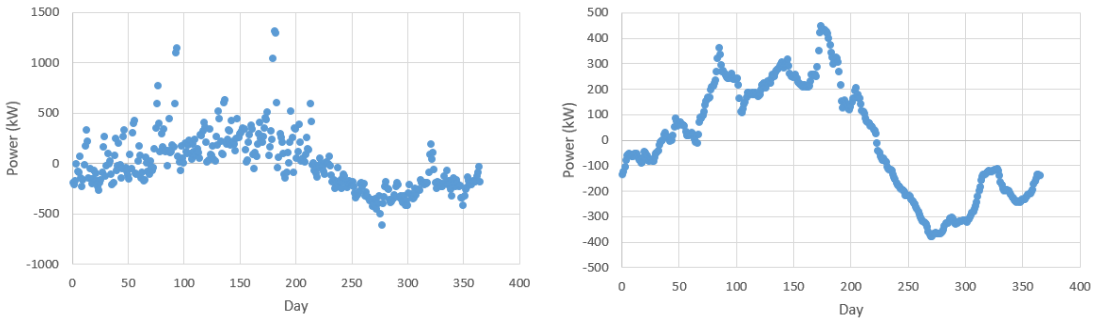

(a) Balanced daily average power demand (b) 19 days moving average

Figure 32 Input daily power profile (balanced case)

For comparison, another set of simulations is conducted with a slightly unbalanced power demand, as shown in Figure 33. The average daily power demand throughout the year is 105 kW, which means there are more heat is injected into the ground than extracted.

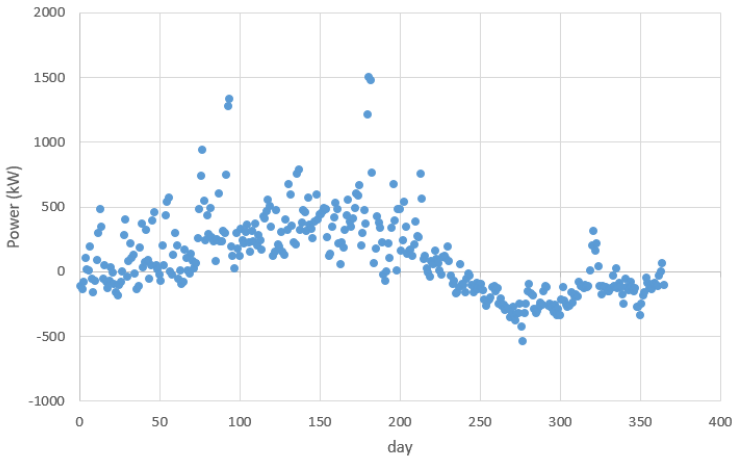

Figure 33 Slightly unbalanced daily average power demand

The total simulation time is 20 years for each case. As the time interval is 20 days, only part of the data points in the daily loading profile are sampled and used in the simulation, as Fig. 34 shows. The finite element code developed by Sun et al. (2021) with the deal.II library (Arndt et al., 2020) is used to conduct the simulation.

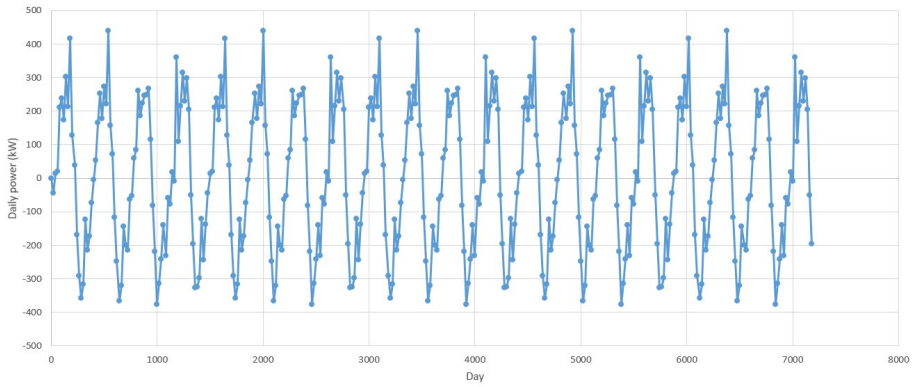

Figure 34 Samples point of daily power value used in simulation for balanced case

5.4.1.2 Simulation results and discussion

The computed temperature contours that cut through the borehole region at the end of the 20th year of the balanced case are shown in Figure 35 for the permeability of k = 1e-9 m/s condition and Figure 36 for the permeability of k = 1e-6 m/s condition. Figure 37 shows the temperature variation along the cross section profile A-A' (see Figure 27) at 100 m depth inside the borehole area. Figure 38 shows the temperature variation along depth, of the point near A, on line A-A', 20 m away from the edge of the borehole area. The plots show that the influence of GSHP operation on the ground temperature of the surrounding region of the borehole area is small and nearly can be ignored (0.1 °C at most). This is due to the fact that the input heat flux values are the differences of the daily heating and cooling demands, which has a relatively lower magnitude. The amount of heat injection and extraction are nearly the same. The temperature at the borehole area increases around 0.5 °C at the end of 20th year; this is due to the sampling results of input heat flux (Figure 34). Resulting average daily power throughout the 20 years of these selected points is around 5kW, which means there is slightly more heat injected than extracted. Thus, the resulting temperatures at the borehole area increases with time but this error is relatively small.

The difference between (a) and (b) of Figure 37 and 38 shows the influence of ground water. As the elevation is higher at the northeast corner of this model and due to the way in assigning the initial conditions mentioned previously, the water pressure and ground temperature are also higher at the northeast part. The heat is transferred to the southwest part of the model by the convection (mainly by advection) of ground water. Thus, the case with higher permeability shows the ambient temperature increases with time.

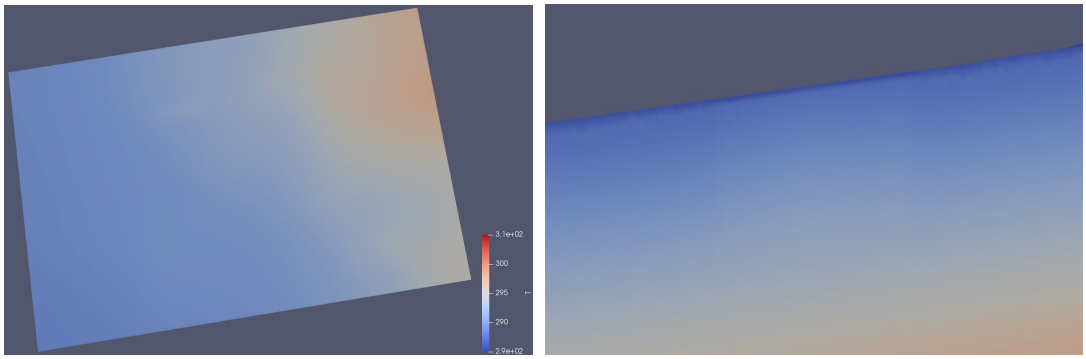

(a) Top view of horizontal clip cut at sea level **(b) Cross sectional profile through A-A'**

Figure 35 Balanced load on low permeability case (k = 1e-9 m/s) at t = 20 years

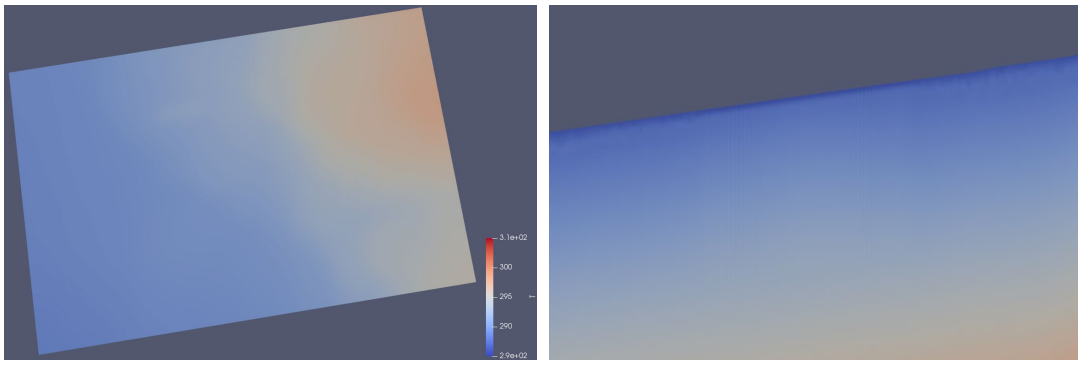

(a) Top view of horizontal clip cut at sea level (b) Cross sectional profile through A-A'

Figure 36 Balanced load on high permeability case (k = 1e-6 m/s) at t = 20 years

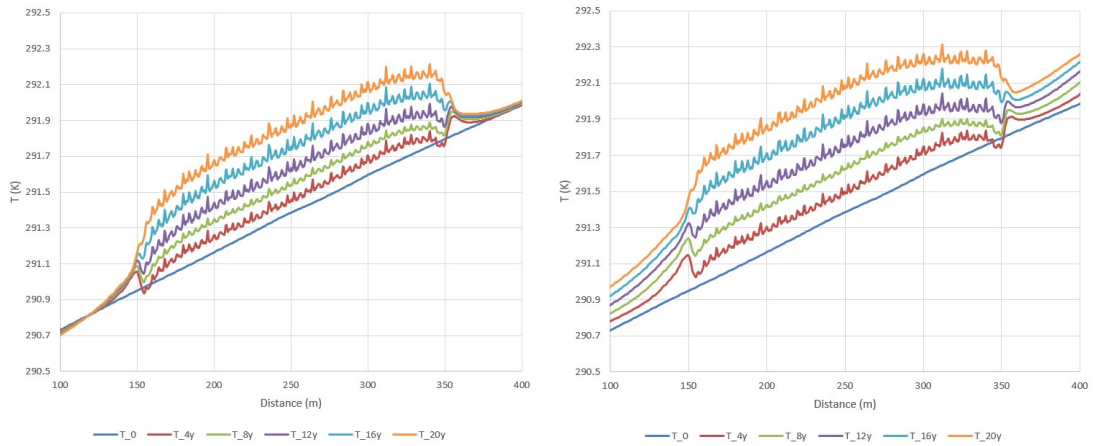

(a) Low permeability case (k = 1e-9 m/s) (b) High permeability case (k = 1e-6 m/s)

Figure 37 Temperature profile along A-A' at 100m depth under balanced load

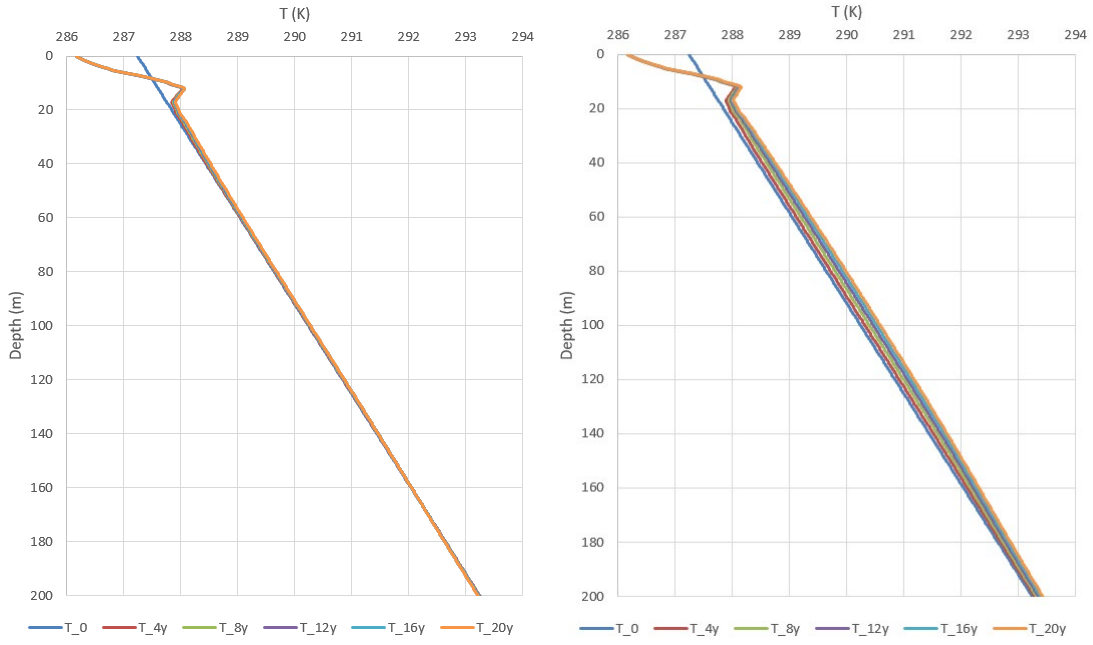

(a) Low permeability case (k = 1e-9 m/s) (b) High permeability case (k = 1e-6 m/s)

Figure 38 Temperature profile along depth at 20m away from borehole area under balanced load

For the cases under unbalanced loading conditions, Figures 39 and 40 show the contours of the temperature profile that cuts through the borehole region at the end of the 20th year. The temperatures of the boreholes increase around 8 °C at the end of the 20th year. Figure 41 shows the temperature variation along the cross section A-A' at 100 m depth. Figure 42 shows the temperature variation along depth at the same location mentioned above. As there is substantially more heat injection than extraction in this case, Figure 42 (b) shows the effect of convection on the heat flux. Borehole temperatures are higher at the western part, as the injected heat is also transferred to southwest by the ground water flow.

According to the small temperature variation (approximately 0.5 °C) around the borehole under balanced load case (Figure 37), this GSHP design does not efficiently use the ground for heat storage. This is because the conventional GSHP system provides heating and cooling separately, and leads the borehole length much longer, which results in the temperature variation caused by the net load much smaller than the allowable value of the ground.

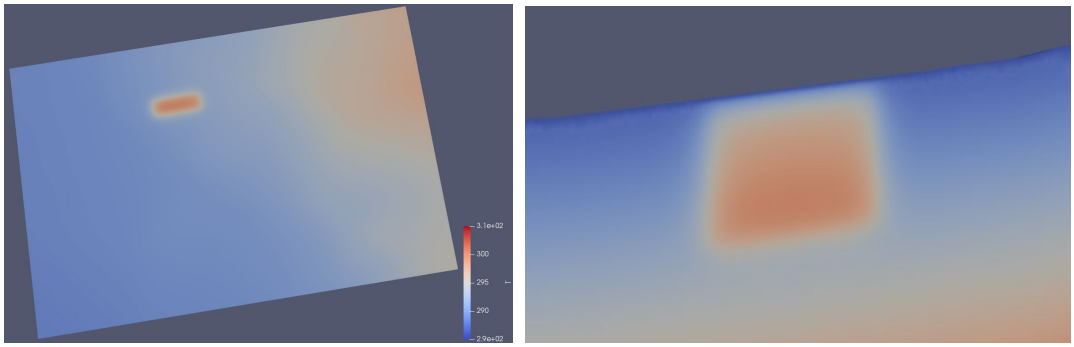

(a) Top view of horizontal clip cut at sea level (b) Side view of clip cut through A-A'

Figure 39 Unbalanced load on low permeability case (k = 1e-9 m/s) at t = 20 years

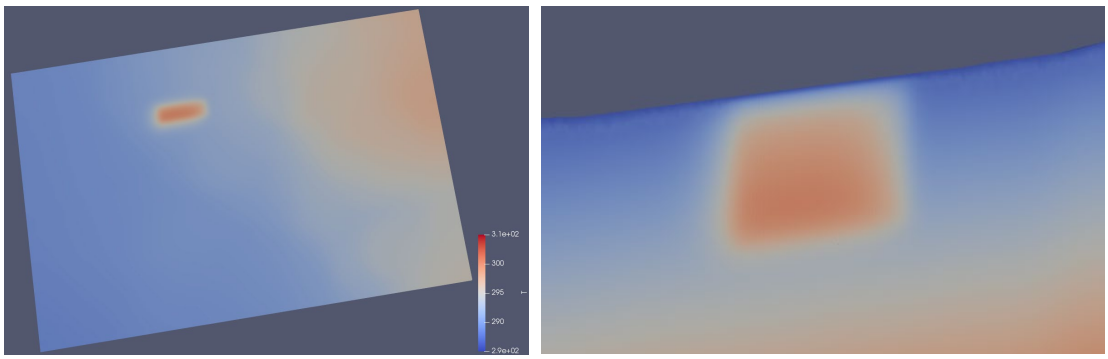

(a) Top view of horizontal clip cut at sea level (b) Side view of clip cut through A-A'

Figure 40 Unbalanced load on high permeability case (k = 1e-6 m/s) at t = 20 years

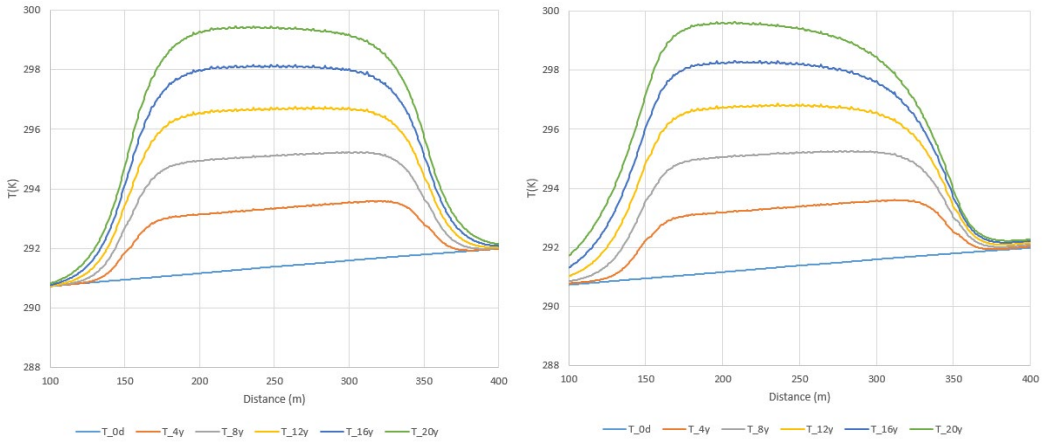

(a) Low permeability case (k = 1e-9 m/s) **(b) High permeability case (k = 1e-6 m/s)**

Figure 41 Temperature profile along A-A' at 100m depth under unbalanced load

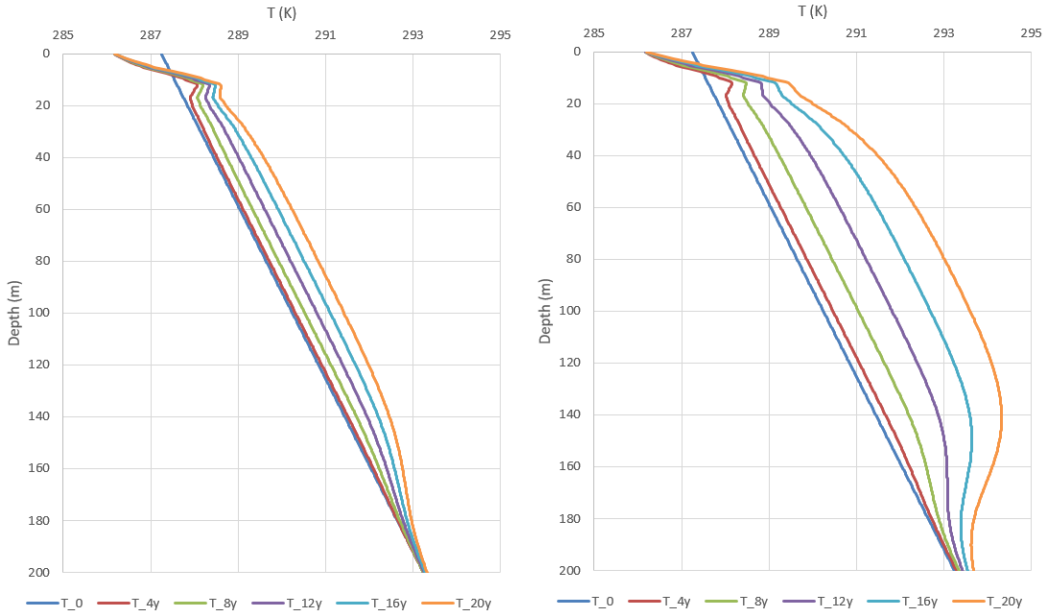

(a) Low permeability case (k = 1e-9 m/s) **(b) High permeability case (k = 1e-6 m/s)**

Figure 42 Temperature profile along depth at 20m away from borehole area under unbalanced load

5.4.2 Model 2

5.4.2.1 Borehole arrangement and loading profile

In this model, there are 203 boreholes in total, each 180 m in length. This represents the central GSHP design (Option 1 and 2) described in Section 4. These boreholes are arranged in a 138 m by 48 m rectangular configuration in 9 rows. Each row has 24 boreholes, except the last one, with has 11 boreholes. The spacing between adjacent boreholes is 6 m.

The building daily power demand for one year is shown below in Figure 43(a). To eliminate the effect of some extreme values, the moving averages with 19 days period are taken, as shown in Figure 43(b). The heating and cooling demands are approximately balanced, and the average value throughout the year is small (-9.48e-6 kW). Using the data shown in Figure 43, Case 1, which is the base case, was

developed for a case that considers an overall ground energy change to be nearly zero. Figure 44(a1) shows the actual data points of daily power that are sampled and used in the simulation, whereas Figure 44(a2) shows the corresponding total energy input into the ground.

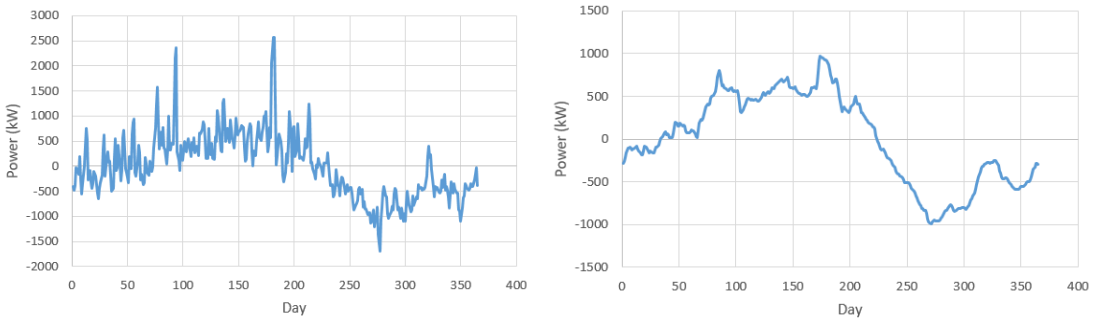

(a) Balanced daily average power demand **(b) 19 days moving average**

Figure 43 Balanced daily average power demand from building simulation

As shown in Table 12, cases with different daily powers and total energy inputs are simulated in this study. The magnitudes of annual variation in power demand in Cases 2, 3, 4 and 5 are x2, x4, x6 and x8 of the magnitude of Case 1. This is to examine the effect of power input on seasonal ground temperature changes. The range of the potential short term peak load to the ground should be from 1000 to 6000 kW, which can be studied in Cases 2, 3 and 4. For the extreme load condition like 8000 kW can also be studied in Case 5. Case 6 considers a scenario where there is slightly more energy injected into than extracted from the ground in each circle (cooling-demand dominated), whereas Case 8 considers a larger imbalanced system (twice of Case 6). Both Cases 6 and 8 have the same annual variation in power demand. Case 7 considers x2 of both energy amplitude and energy imbalance of Case 6. Case 9 is a scenario where there is slightly less energy injected into than extracted from the ground in each circle (heating-demand dominated). Case 10 considers x2 of both energy amplitude and energy imbalance of Case 9. In Figure 44, the power histories of Case 1, 6 and 9 are presented as examples. All the cases have similar power history configurations, which can be characterized by the energy amplitude and amount of energy imbalance as shown in Figure 44d. The parameters for the twelve cases are listed in Table 12.

Table 12 Summary of input loading cases

Case	Energy amplitude ((Max-Min)/2) (kJ)	Energy imbalance (error) in each circle (kJ)	Error percentage error/(2*amplitude) (%)
1	9.81E+05	-6.82E+02	-0.035
2	1.96E+06	-1.36E+03	-0.035
3	3.92E+06	-2.73E+03	-0.035
4	5.89E+06	-4.09E+03	-0.035
5	7.85E+06	-5.45E+03	-0.035
6	1.00E+06	4.51E+04	2.244
7	2.01E+06	9.01E+04	2.244
8	1.03E+06	9.08E+04	4.421
9	9.50E+05	-6.21E+04	-3.270
10	1.90E+06	-1.24E+05	-3.270

(a1) Case 1

Daily power

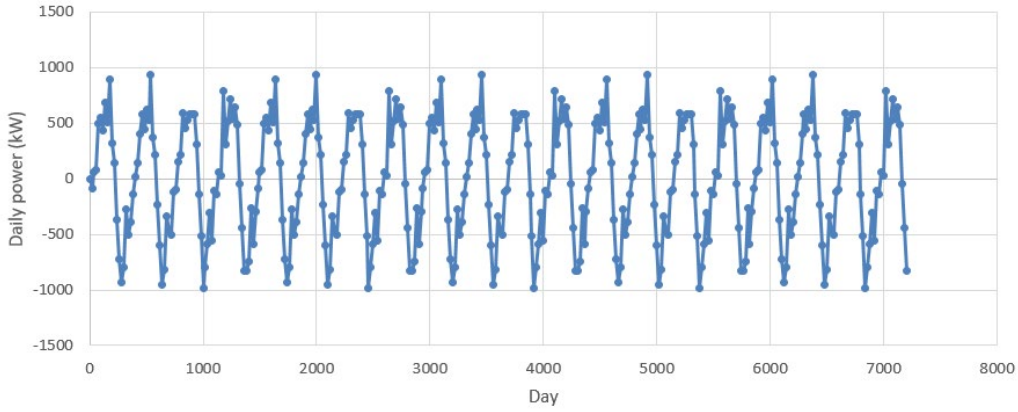

(a2) Case 1

Energy input

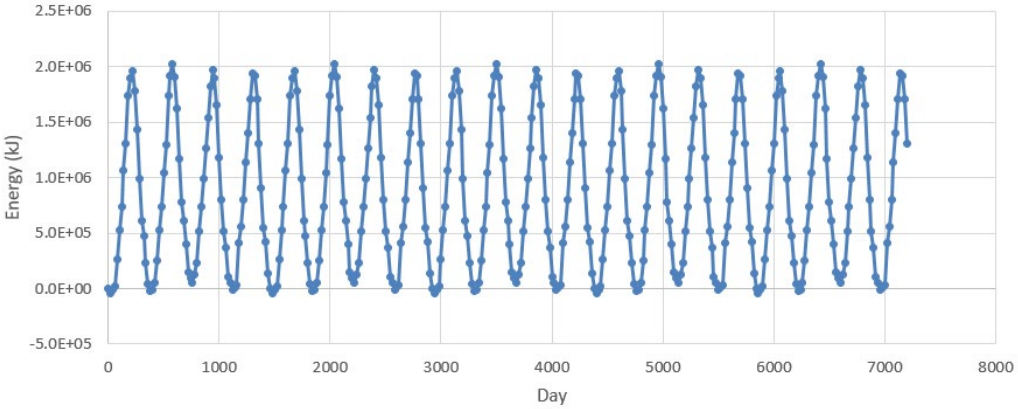

(b1) Case 6

Daily power

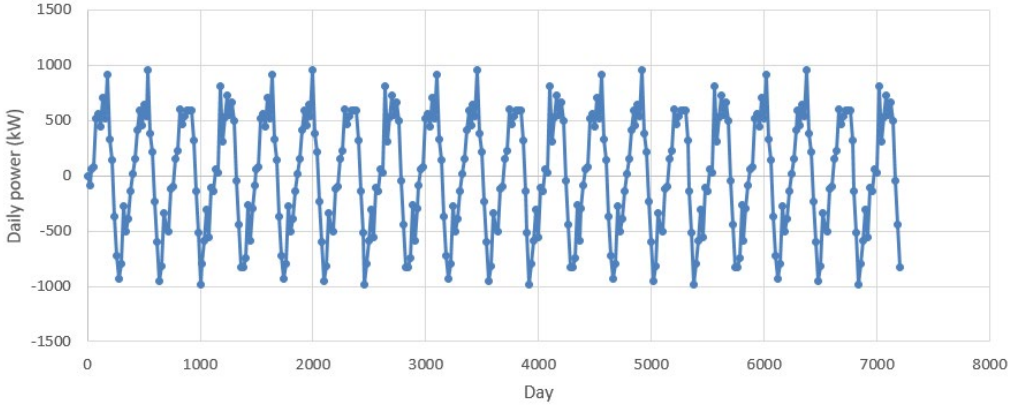

(b2) Case 6

Energy input

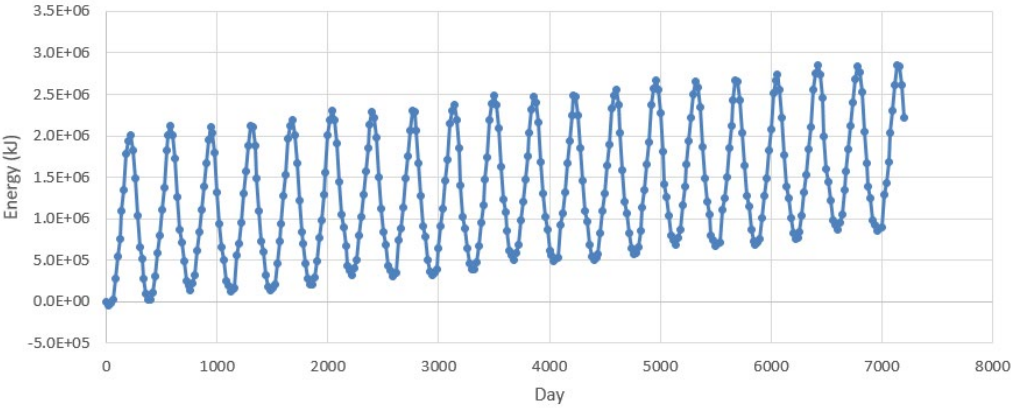

Figure 44 Input daily power and total energy profile for each case

(c1) Case 9

Daily power

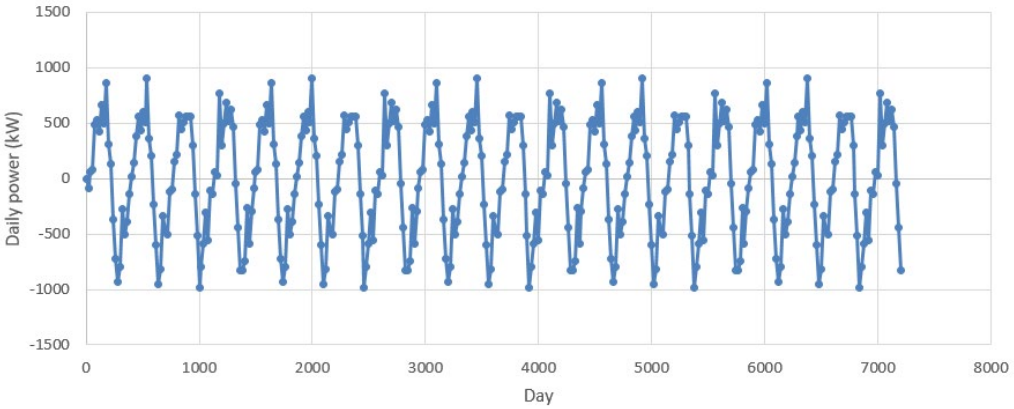

(c2) Case 9

Energy input

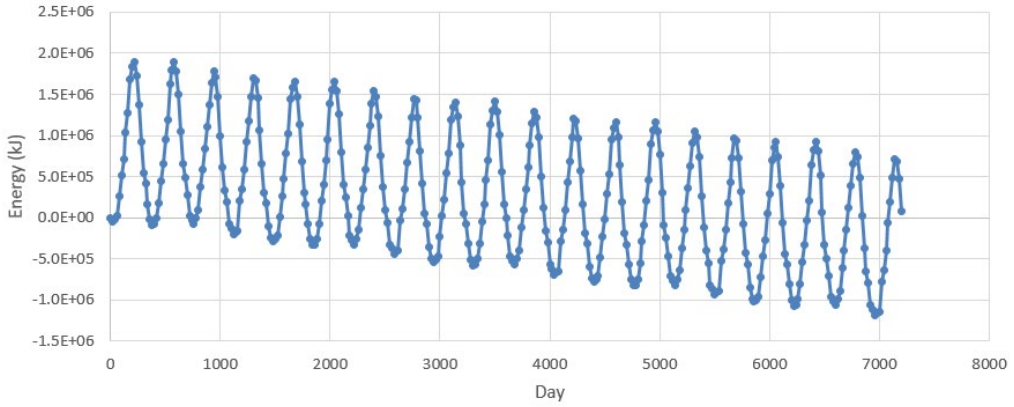

(d) Sketch of

Energy input

history

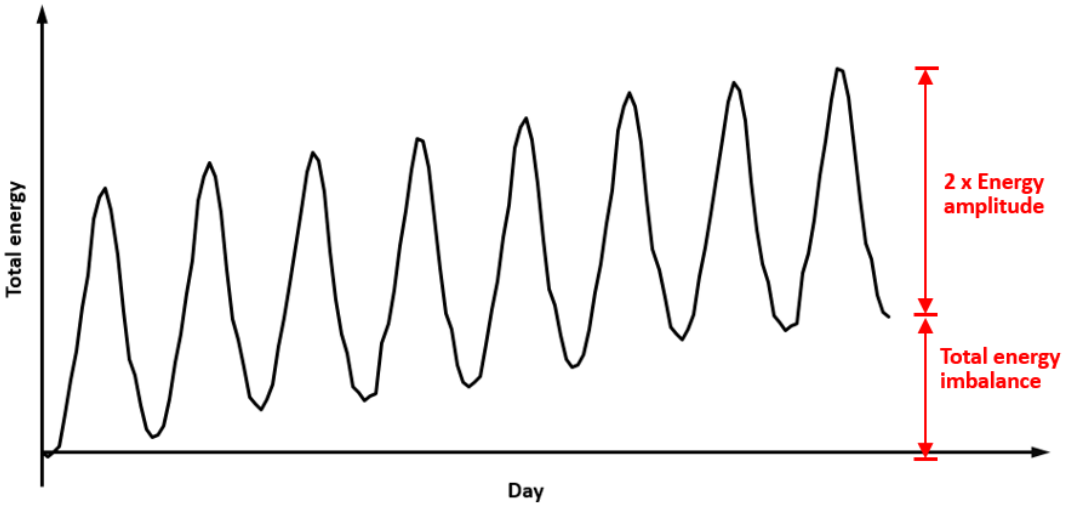

Figure 44 Input daily power and total energy profile for each case (cont.)

5.4.2.2 Simulation results and discussion

The simulation temperature profiles across the borehole area, at around 100 m depth, for Case 1, 2, 6, 9 are shown in Figure 45, and the profiles of the other cases have similar configurations. The borehole area is in between 150 m to 300 m of x axis. As there are large temperature variations near borehole, there are lots of spikes in this range. The downward spikes are much larger in April, which is the end of heating season that the heat keeps being extracted from the ground. Similarly, much larger upward spikes appear in October, which is the end of cooling season. The borehole area influences the ground temperature of its surrounding region (within around 25 m).

Effect of groundwater

The northeast side of the model has a higher elevation water table and initial temperature and hence the groundwater flows toward the southwest throughout the area. This affects the temperature profiles in two ways. First, the groundwater brings extra heat from upstream to this area, which increases the background temperature. As shown in Figure 45, in the locations that are relatively far away (in 50-100m and 350-400m of the x-axis) and have not been affected by the borehole, the temperature profiles have small constant increments with time in the high permeability cases. In contrast, for the low permeability cases, the temperatures far away nearly remain constant. Second, the groundwater flow affects the temperature field caused by the heat flux from the boreholes. The heat at the eastern part is brought to the western part of the borehole area by advection. The western part heats up faster and cools down slower compared to the eastern part under the effect of lateral groundwater flow. This is also shown in Figure 45 by comparing the plots for the same loading case but with different permeabilities (plot 1 vs 3, or 2 vs 4). The high permeability cases give higher temperatures at the western location.

Effect of imbalance (Case 1 vs Case 6 vs Case 9)

Figure 46 shows the temperature histories of the point at the middle of the borehole area, at around 100 m depth for Cases 1, 6 and 9, which have different heat imbalance magnitudes. Its distance to the adjacent borehole is 3 m. Only low permeability cases are plotted here. As discussed above, the low permeability cases are less affected by the ground water flow, and thus they are used to investigate the effect of input energy on the resulting ground temperature profiles.

In Case 1, the amount of energy imbalance in each year is -6.82e2 kJ (equivalent average daily power -0.078 kW); this results in a 0.005 °C average change in the ground temperature each year. The amplitude of energy in this case is 9.8e5 kJ, which results in a 0.9 °C amplitude of the temperature profile. There is a small amount of positive average temperature change each year even through under a negative daily power input. This may be due to the ground water flow that brings extra heat to this area. In Case 6, the amount of energy imbalance occurring each year is 4.51e4 kJ (equivalent average daily power 5.148 kW), resulting in a 0.027 °C average increment of ground temperature near the borehole area each year. The amplitude of energy in this case is about 1e6 kJ, which results in a 0.9 °C amplitude of temperature profile. In Case 9, the amount of energy imbalance in each year is -6.21e4 kJ (equivalent average daily power -7.089 kW), and this makes the ground temperature at the borehole area decrease by 0.042 °C on average each year. The amplitude of energy in this case is about 9.5e5 kJ, which results in a 0.9 °C amplitude of temperature profile as well. These three cases have similar energy fluctuations (around 9.8e5 kJ in amplitude), and hence result in similar degrees of ground temperature fluctuation in one year (around 0.9 °C in amplitude).

(a1) Case 1

Low permeability

April

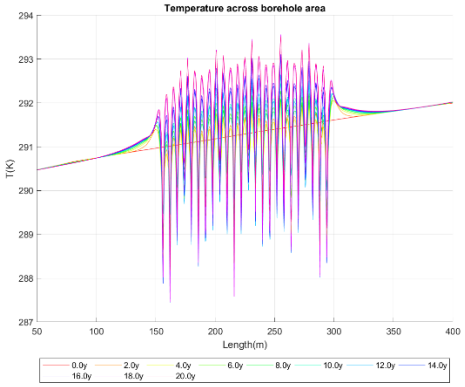

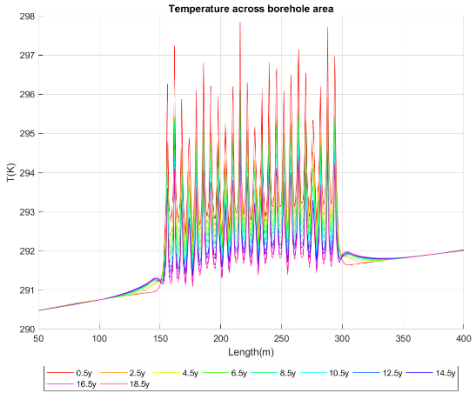

(a2) Case 1

Low permeability

October

(a3) Case 1

High permeability

April

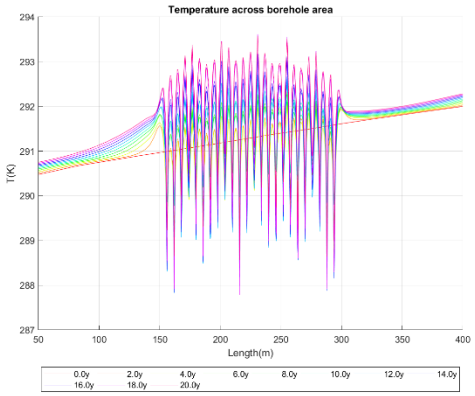

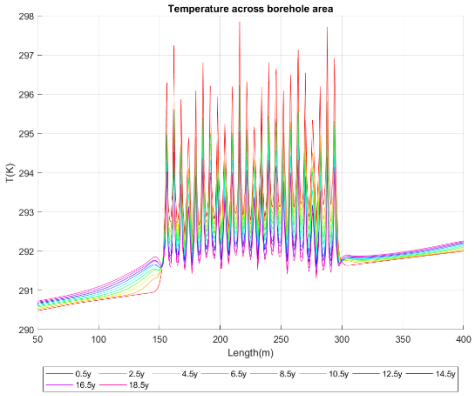

(a4) Case 1

High permeability

October

(b1) Case 2

Low permeability

April

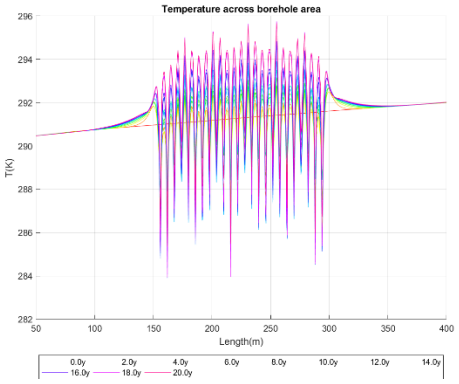

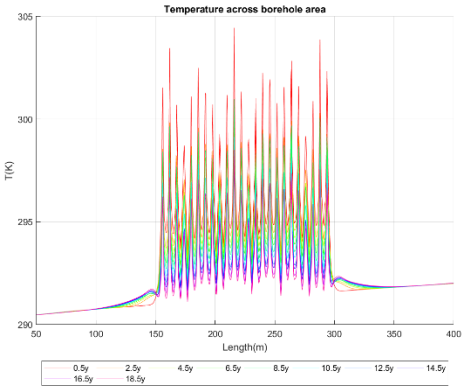

(b2) Case 2

Low permeability

October

(b3) Case 2

High permeability

April

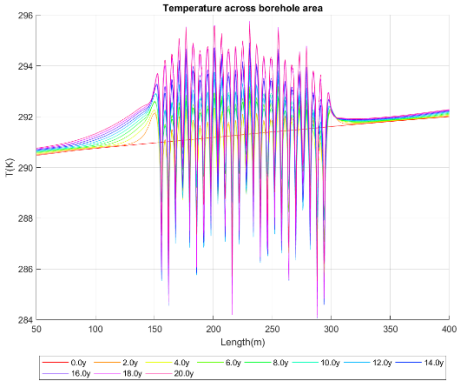

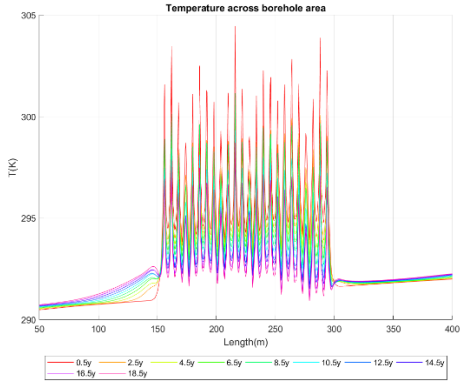

(b4) Case 2

High permeability

October

Figure 45 Resulting temperature profile across borehole area (section A-A')

(c1) Case 6

Low permeability

April

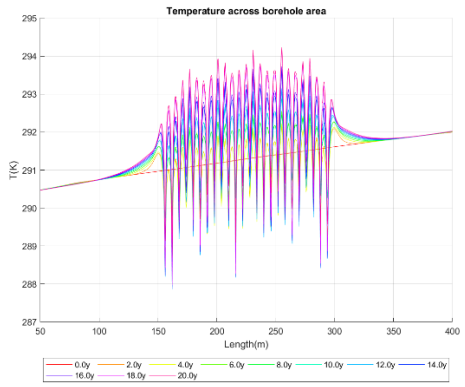

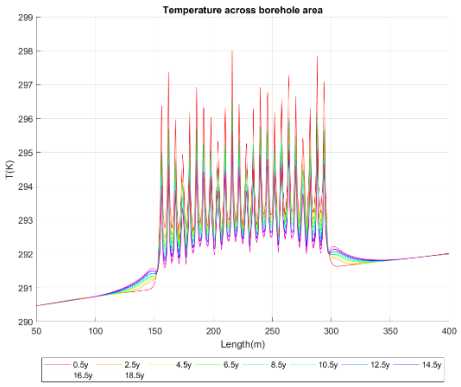

(c2) Case 6

Low permeability

October

(c3) Case 6

High permeability

April

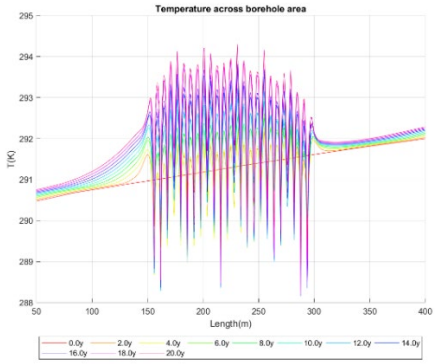

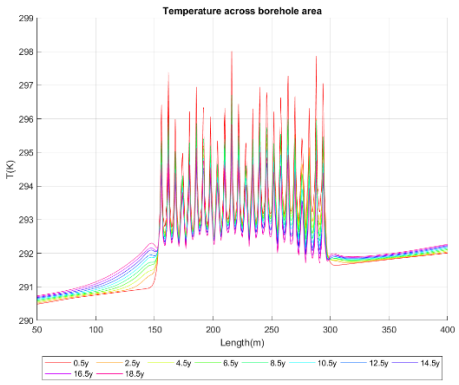

(c4) Case 6

High permeability

October

(d1) Case 9

Low permeability

April

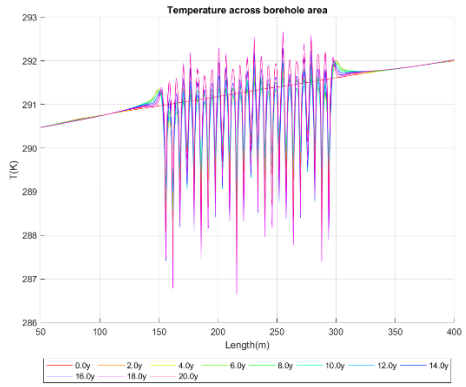

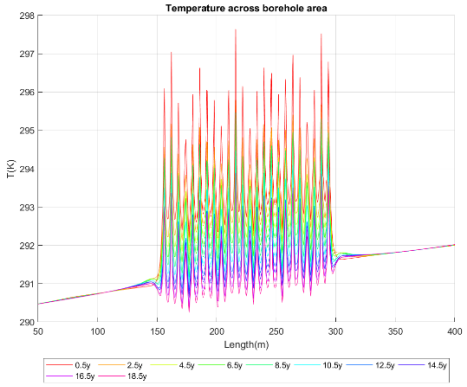

(d2) Case 9

Low permeability

October

(d3) Case 9

High permeability

April

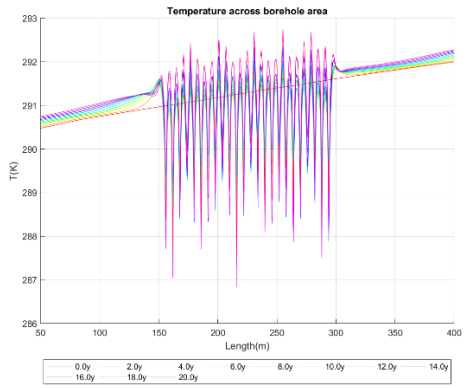

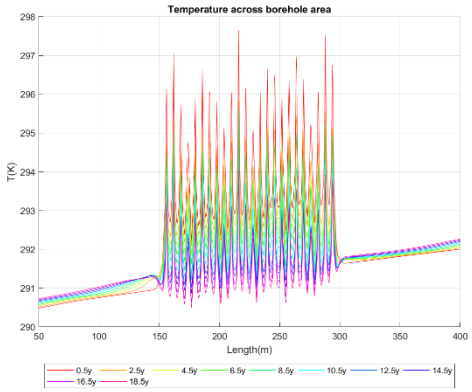

(d4) Case 9

High permeability

October

Figure 45 Resulting temperature profile across borehole area (section A-A') (cont.)

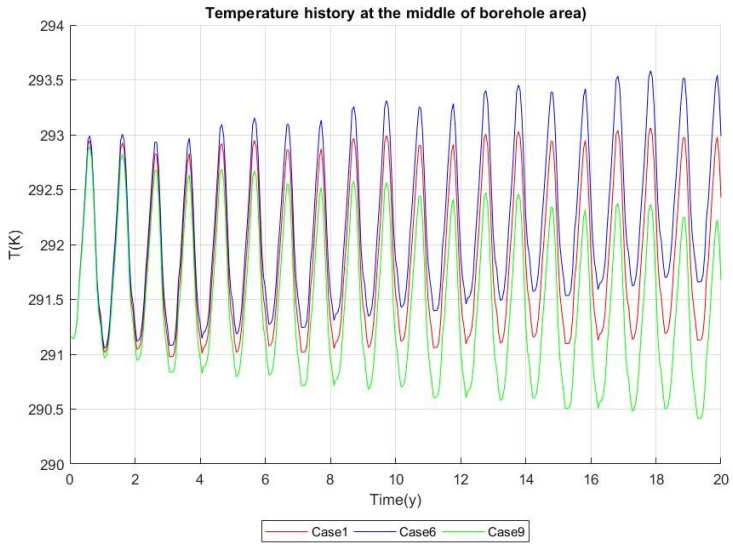

Figure 46 Ground temperature history at the middle of borehole area (Case 1, 6, 9)

Effect of energy amplitude (Cases 1-5; Case 6 vs Case 7; Case 9 vs Case 10)

As shown in Figure 47, for these balanced loading cases, the amplitude of temperature change is around 0.9 °C, 1.8 °C, 3.6 °C, 5.4 °C and 7.25 °C for Cases 1-5, respectively. The amplitudes of Cases 2-5 are 2, 4, 6, and 8 times the amplitude of Case 1, respectively. In this simulated temperature range, the temperature variation is approximately linearly influenced by the input energy variation. Figure 48 compares Cases 6 and 7, which are imbalanced cases with positive energy accumulated in the ground. The amplitudes of temperature profile are 0.93 °C and 1.85 °C for Cases 6 and 7, respectively. They have a 0.027 °C and 0.055 °C average annual temperature increments, which are reasonable as the amount of imbalance is also doubled. Figure 49 compares Cases 9 and 10, which are imbalanced cases with more energy extracted from the ground. The amplitudes of temperature profile are 0.88 °C and 1.75 °C for Cases 9 and 10, respectively, and the average annual increments are -0.038 °C and -0.072 °C. In summary, for both balanced and imbalanced cases, the temperature profiles vary linearly with the input energy profiles.

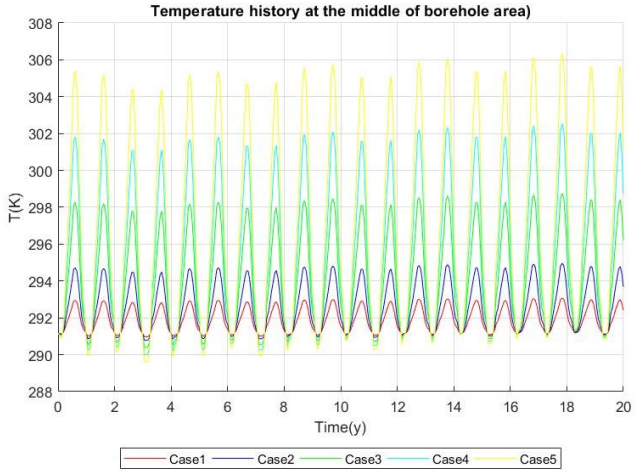

Figure 47 Ground temperature history at the middle of borehole area (Case 1-5)

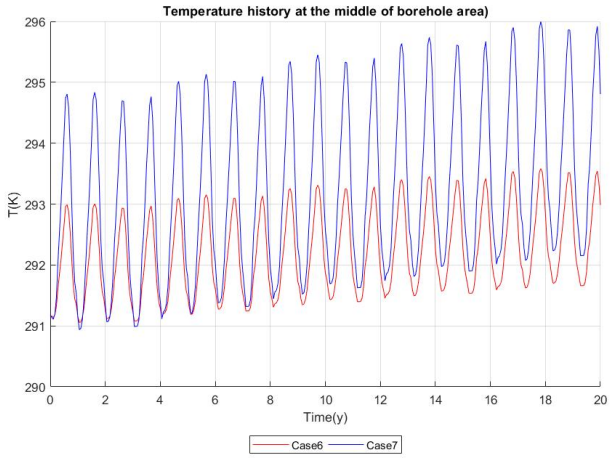

Figure 48 Ground temperature history at the middle of borehole area (Case 6, 7)

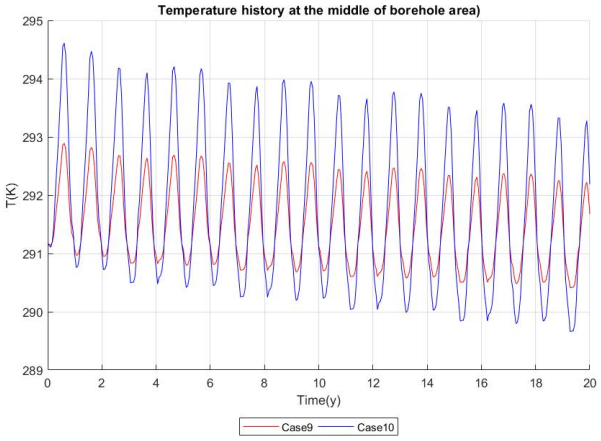

Figure 49 Ground temperature history at the middle of borehole area (Case 9, 10)

In order to show this linear relation more explicitly, the resulting temperature histories of Cases 2-5 are normalized to the magnitude of Case 1 by linearly scaling them using the amplitude of the first cycle. Figure 50 shows that these normalized temperature histories are very similar. Similarly, Case 7 and Case 10 are normalized to the magnitudes of Case 6 and Case 9, respectively, and plotted in Figures 51 and 52.

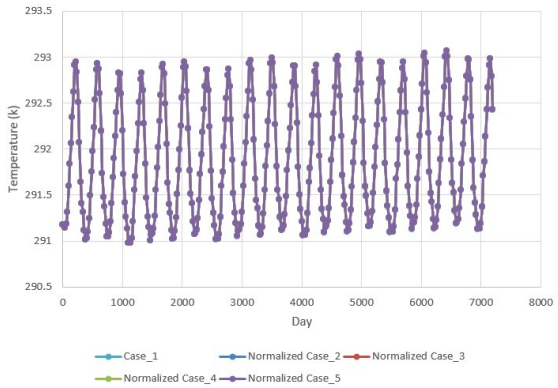

Figure 50 Normalized temperature history at the middle of borehole area (Cases 1-5)

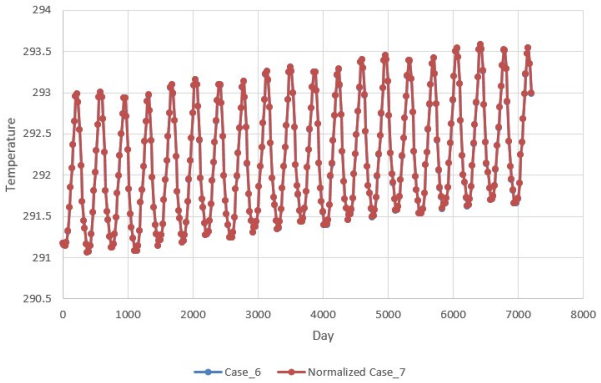

Figure 51 Normalized temperature history at the middle of borehole area (Cases 6, 7)

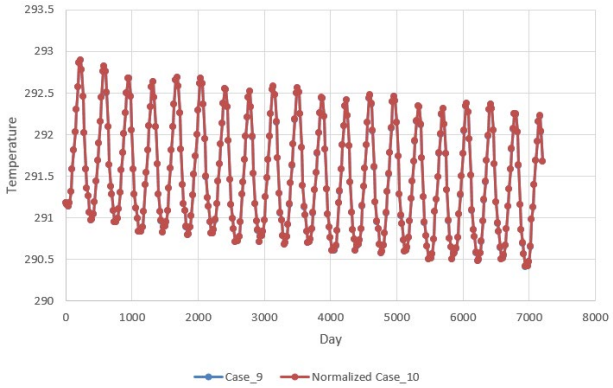

Figure 52 Normalized temperature history at the middle of borehole area (Cases 9, 10)

Relationship between ground temperature and input energy

Figure 53 shows that the ground temperature profile is approximately linearly related with the input energy profile. In Cases 9 and 10, as the energy is extracted, the temperature tends to decrease in each circle. But the heat brought by lateral ground water flow slightly counters this effect and this causes the data points to slightly shift upward. In Cases 1-5, although their annual input energies are nearly zero in each period, the data points are also slightly shifted upward after each period. This effect is more apparent for the cases with larger magnitude of energy input and the reason for this is currently being investigated.

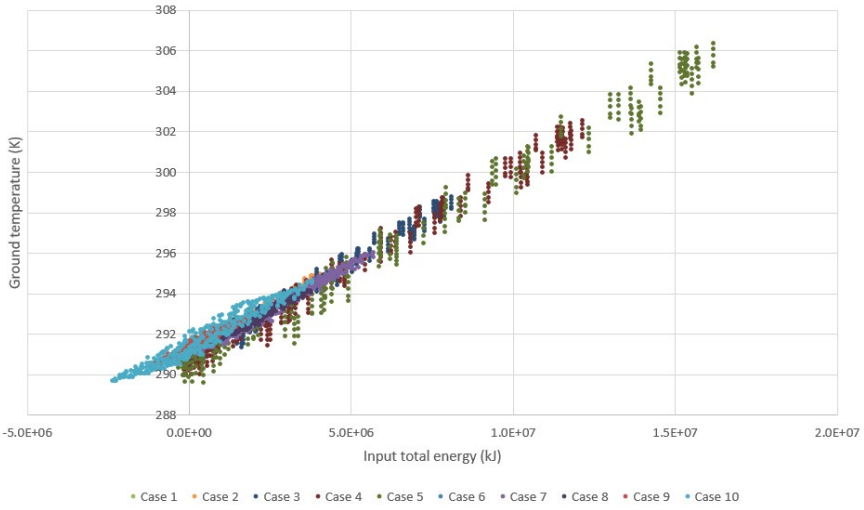

Figure 53 Ground temperature vs input total energy

In order to investigate the effect of different loading cases to the efficiency of GSHP, the data points in Figure 53 are grouped and plotted in Figures 54-56 for different sets of loading cases. Figure 54 shows the balanced cases (Case 1 to 5). The temperature at peak loading for each case is marked. As the energy input is balanced throughout the year, for each case, the maximum and minimum temperatures are nearly the same every cycle. The minimum temperature is approximately 291 K for all the cases, which is the initial temperature. The relation of maximum temperatures among these cases are coincident with the magnitude of input loading.

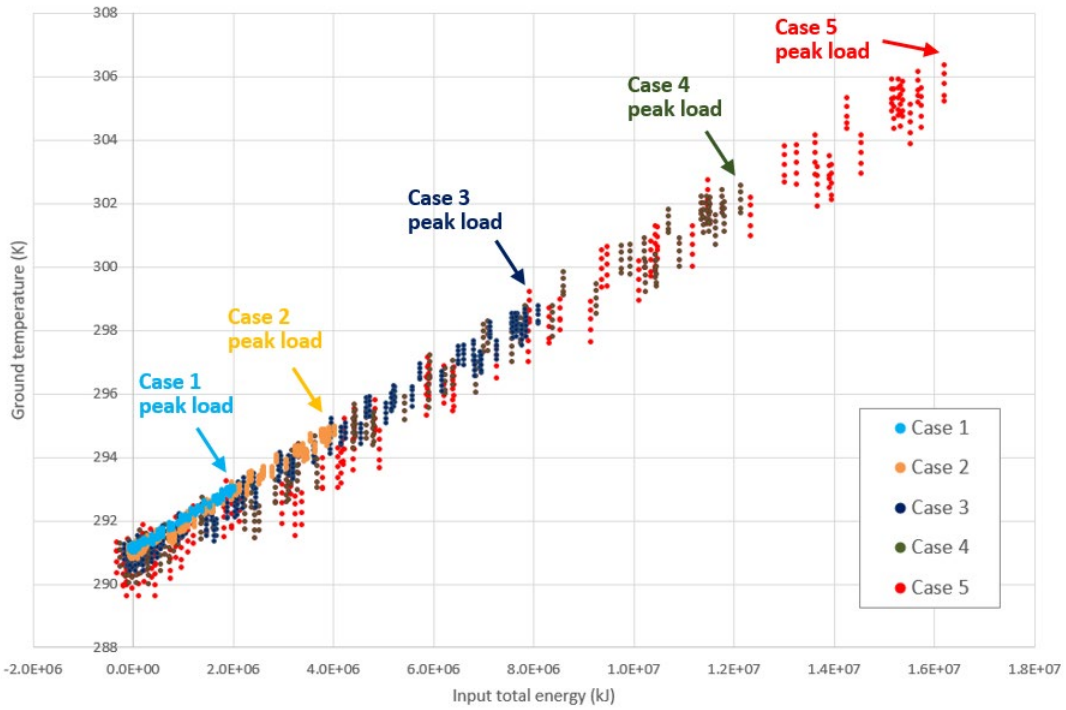

Figure 54 Ground temperature vs input total energy (Case 1-5)

Figures 55 and 56 show the imbalanced cases under excessive heat injection and extraction, respectively. The ranges of temperature for the 1st and 20th year are marked in the figures for all the cases. The upper and lower ends of the range represent the maximum and minimum temperatures achieved in this cycle. In Figure 55, as there is more energy injected into the ground, the cycles shift to the right (larger range of accumulated energy) and upward (higher range of temperature) every year. As the energy fluctuation is approximately the same throughout the year for the same case, the difference between the maximum and minimum temperatures (length of the cycle) remains the same for every annual cycle. Similarly, in Figure 56, as the energy is extracted from the ground every year, the cycles shift to the left (less accumulated energy) and downward (lower range of temperature), while the difference between the maximum and minimum temperatures remains the same for every cycle as well. The amount of shifting and length of each cycle are proportional to the energy amplitude and amount of energy imbalance.

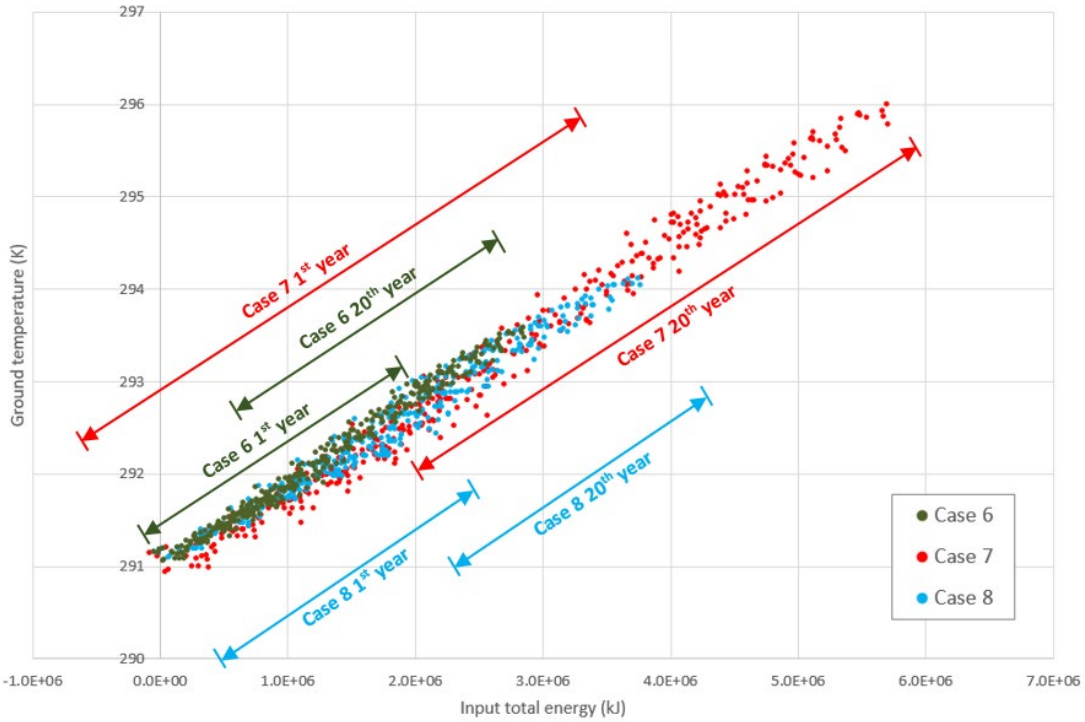

Figure 55 Ground temperature vs input total energy (Case 6-8)

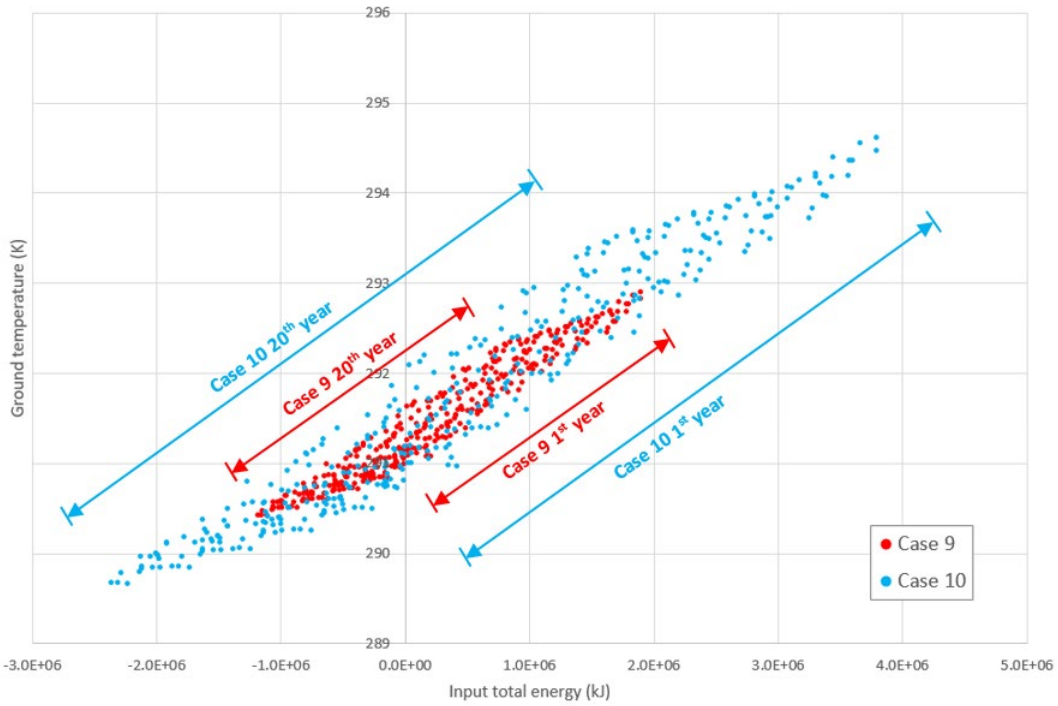

Figure 56 Ground temperature vs input total energy (Case 9, 10)

The rate of imbalance affects the ground temperature over time. Figure 57 shows the temperature vs the amount of energy imbalance per year for all the imbalanced loading cases. In order to better visualize the change of the temperature range, cases with similar magnitudes of energy amplitude are plotted together. The circular data points connected with solid lines represent the maximum and

minimum temperature at the 1st year, while the triangular data points connected with dash lines represent those at the 20th year. Therefore, the lines represent the range of ground temperature throughout the year. The initial temperatures for all the cases are approximately 291 K (the lower circular points).

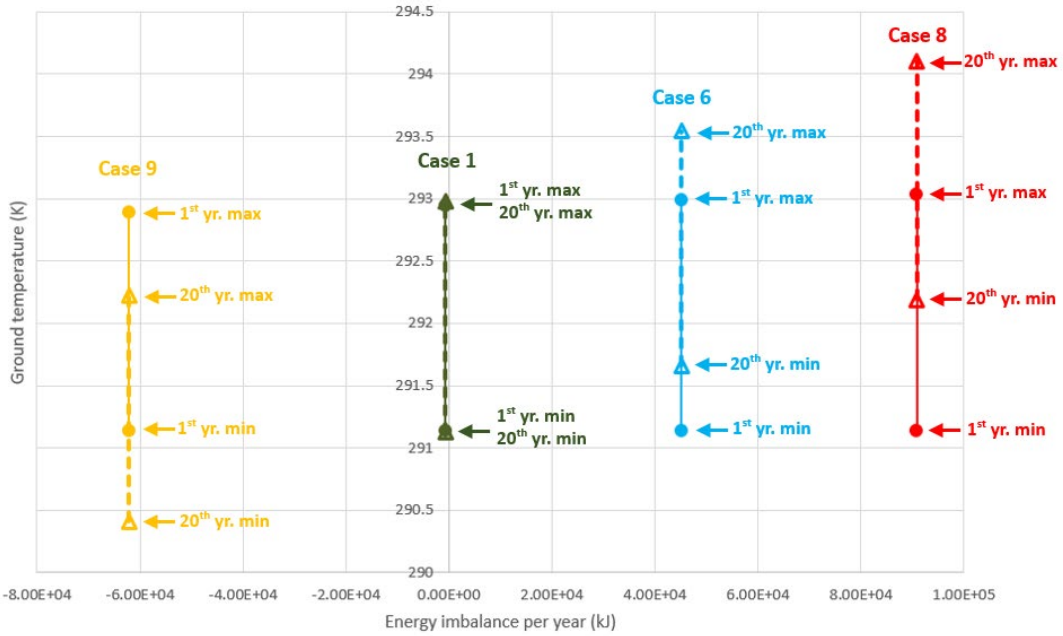

(a) For Case 1, 6, 8, 9 (cases with similar energy amplitude as Case 1)

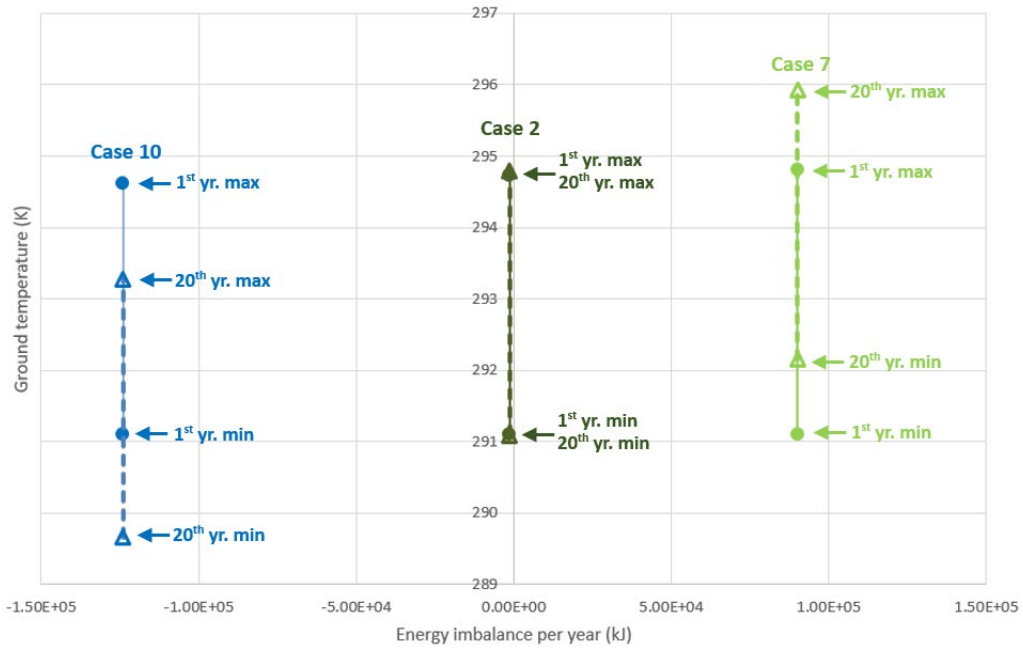

(b) For Case 2, 7, 10 (cases with around 2 * energy amplitude of Case 1)

Figure 57 Ground temperature vs amount of energy imbalance per year

In Figure 57a, Case 6, 8, 9 have similar values of energy amplitude as Case 1 (the base case). Their range of 1st year's ground temperature are nearly the same, and thus they have similar maximum temperature (upper circular points). Similarly, Case 2, 7 and 10 (Figure 57b) have twice energy amplitude of Case 1, and thus their 1st year's temperature ranges are doubled. According to the triangular data points (for the 20th year), for the energy injection cases (Case 6, 8 in Figure 57a and Case 7 in Figure 57b) with positive energy imbalance, the ranges of temperature shift upward (temperature increases) with time. The amount of shifting is proportional to the amount of energy imbalance. While the difference between maximum and minimum values (the lengths of solid and dash lines) keeps nearly the same, the energy amplitudes do not change with time. Case 7 and 8 have similar amount of energy imbalance with similar amount of shifting (approximately 1.1 °C). Therefore, they have similar start points in both the 1st year and 20th year cycle (minimum temperature, which is represented by the lower circular and triangular data points). For the energy extraction cases (Case 9 in Figure 57a and Case 10 in Figure 57b) with negative energy imbalance, the ranges of temperature shift downward (temperature decreases) with time.

5.5 Potential influence of the simulated ground temperature changes on GSHP COP

Different heat pumps, different condensation and evaporation conditions lead to different COP values. Some manufacturers report several COP values for one model under various conditions (Qian et al., 2013) and Staffell et al. (2012) report an empirical equation that shows a temperature dependent COP (see Figure 58).

$$COP_{GSHP} = 0.000734\Delta T^2 - 0.15\Delta T + 8.77$$

where ΔT is the temperature difference between heat pump heat source and heat sink, and its value should be between 20℃ and 60℃.

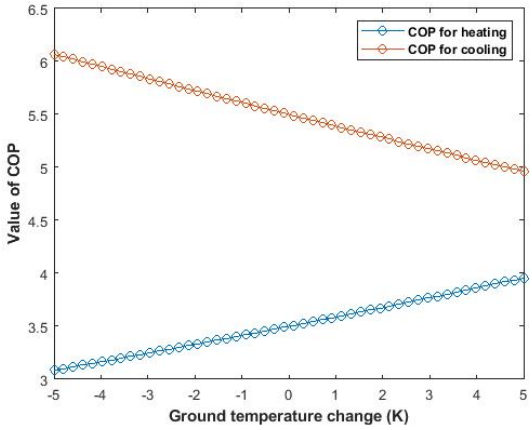

Figure 58 COP vs ground temperature change

In the GSHP design presented earlier, the heating hot water supply temperature in winter is 60℃ (average sink temperature 57.5℃) and the chilled water supply temperature in summer is 3.3℃ (average source temperature 5.9℃). The average ground loop temperature in the heating mode is 5.5℃ and that in the cooling mode is 27.5℃. As the ground temperature increases, the heating COP increases and the cooling COP decreases. Because the Bioscience node is cooling dominated, if the loads are imbalanced and the average ground temperature increases, the COP value for cooling decreases and it would further increase the load for the chiller.

Because of the cooling-dominated condition mentioned before, the cooling COP variations after 20

years' operation are estimated based on representative temperatures in the cooling season for Cases 1-10 in Table 13. For the imbalanced condition, since Cases 1, 6, 8 and 9 have similar magnitude of load, 1000 kW is used as the representative load to calculate the electricity consumption increase with respect to the change of cooling COP value. Similarly, 2000 kW is selected as the representative load for Cases 7 and 10. For the balanced condition, 2000 kW, 4000 kW, 6000 kW and 8000 kW are selected as the representative loads for Cases 2-5.

Imbalanced heat extraction conditions like Cases 9 and 10 have higher cooling COP values compared with other cases. This is because the cooled ground has a higher heat dissipation rate around the borehole. However, this imbalanced heat extraction condition would decrease the heating COP value and is not normal in the cooling-dominated Bioscience node. As the load amplitude increases from Cases 1 to 5, the representative temperature in the cooling season increases, and the cooling COP value decreases from 5.4 to 4.7. For Cases 6, 7, 8, all of them are imbalanced heat injection conditions; Case 8 has two times the energy imbalance compared with Case 6, whereas Case 7 has two times of both energy imbalance and amplitude compared with Case 6. In this way, as the representative temperature in the cooling season increases from Cases 6 to 8 then to 7, the cooling COP value decreases from 5.3 to 5.17. According to the ratio between the electricity consumption increase per unit load (ECIPL) for a given case relative to that of Case 1, there is an apparent electricity consumption increase per unit load with load amplitude increase or imbalanced heat injection condition. Therefore, it is important to design the control loop to avoid the load imbalance and load amplitude change condition.

Table 13 COP variation analysis

Case	Initial temperature after 20 years' operation [K]	Average temperature shift in the cooling season (Summer) [K]	Representative temperature in the cooling season [K]	Cooling COP (5.5 in the design condition)	Electricity consumption increase compared with COP 5.5 condition [kW]	Electricity consumption increase per unit load (ECIPL) [kW/kW]	Ratio between ECIPL and ECIPL of Case 1
1	291	0.9	291.9	5.4	3.37	0.0034	1
2	291	1.8	292.8	5.3	13.72	0.0069	2.03
3	291	3.6	294.6	5.1	57	0.0143	4.2
4	291	5.4	296.4	4.9	133.6	0.0223	6.6
5	291	7.25	298.25	4.7	247.6	0.0309	9.1
6	291.54	0.93	292.47	5.3	6.86	0.0069	2.03
7	292.1	1.85	293.95	5.17	23.2	0.0116	3.4
8	292.1	0.95	293.05	5.27	7.9	0.0079	2.32
9	290.24	0.88	291.12	5.49	0.33	0.0003	0.09
10	289.56	1.75	291.31	5.47	2	0.001	0.3

5.6 Computational time cost

In this study, the simulations were performed using Stampede2's Skylake (Intel Xeon Platinum 8160, 96 cores) compute nodes, which is the HPC system at UT Austin. To examine the performance of the simulations, a case of 5 years of simulations with 20-day intervals was run on Model 1 with different numbers of MPI processors. The total computation time cost for each case is shown in Figure 59. When the number of processors is the same, each time step in simulation takes nearly the same amount of time. The results can be linearly scaled for 20 years of simulation.

In this study, the 20-year simulations with 20-day intervals for Model 1 (around 1.9 million elements) and Model 2 (around 1.3 million elements) using 8 MPI processors take approximately 7.5 hours and 5.5 hours respectively. In simulating a finer mesh, if the number of elements is increased but still in the same magnitude, the simulation time may be estimated by linearly scaling current results, and still falls in an acceptable range. But if the mesh is much finer, the code needs to be further parallelized for better

performance.

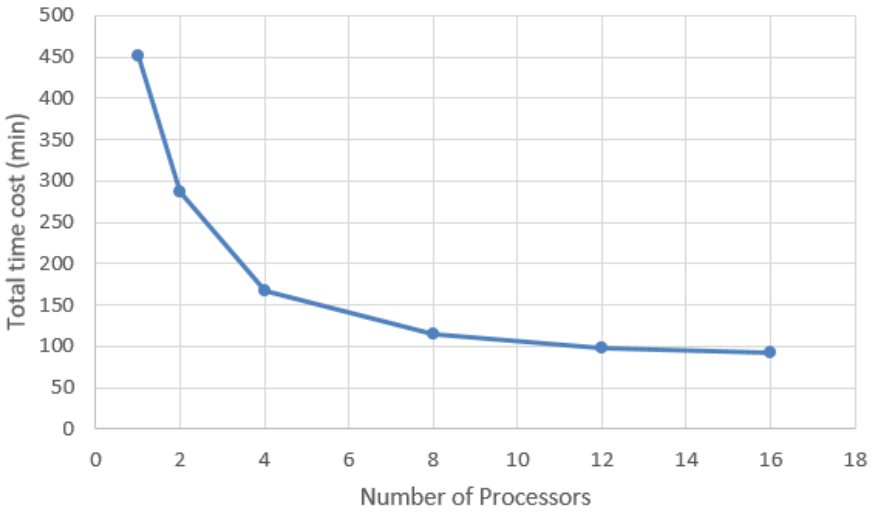

Figure 59 Computation time cost for 5-year simulation with different number of MPI processors

6. CONCLUSIONS

A series of building simulations based on CPBM model approximation was performed to evaluate the load demand of the UCB Bioscience node. Based on the load profiles, several preliminary GSHP designs for the UCB Bioscience node were developed.

- Parametric analysis was carried out to assess the application of GSHP system for this node. Based on the distribution of utility pipelines and available empty area surrounding the potential central plant for the Bioscience node, the space east of University House is identified as one of the potential areas for GSHP installation, where the area is 200 m x 64 m.
- Two load cases are proposed based on each building's metered annual load and peak load data. Three options are proposed for the GSHP design. Option 0 considers the conventional GSHP system, which can provide heating or cooling. For Options 1 and 2, a system that can provide simultaneous heating and cooling is utilized. Options 1 and 2 correspond to two different operation strategies of auxiliary fluid cooler. Six borehole designs are carried out and categorized into two models for the simulation.
- For Option 0, the decrease in boreholes numbers for Load case 2 is because this option considers heating base load and cooling base load separately and the cooling base load, which dominates the design, is larger in Load case 1 than that in Load case 2, which decreases the design lengths of GSHP for Load case 2. For Option 1 and 2, the increase in borehole numbers for Load case 2 is because the difference between the heating base load and the cooling base load is much larger in Load case 2 than that in Load case 1, which increases the net load to the ground and further increases the design lengths of GSHP.
- Potential CO_2 and electricity savings by adopting the GSHP for the Bioscience node were estimated. The annual electricity savings made by choosing the NHR option with GSHP rather than that with ASHP is 314835.84 kWh/year, and the corresponding CO_2 savings before 2045 would be 82.5 tons/year.

The geothermal models of the UCB campus with the primary GSHP designs are built based on the geological data from different sources. The thermal performance of the ground based on several scenarios are studied and a series of sensitivity analysis are performed.

- The groundwater affects the temperature distribution by: 1) bringing extra heat from warmer region via lateral flow driven by a hydraulic head gradient; 2) affecting the temperature field caused by heat flux from borehole.
- For Model 1 (conventional GSHP design), it has a small temperature variation (<1 °C) under the balanced load case. This is because the GSHP is designed to meet the peak cooling load, which is much larger than the net peak load. Therefore, this design gives a larger number of boreholes but with a small heat flux per unit length.
- For Model 2 (central GSHP design), approximately 1e6 kJ energy fluctuation results in 1 °C variations in the temperature profile at the middle of the borehole area. This relationship varies with the borehole design and sampling location. The effect of energy fluctuation on ground temperature decreases as the total borehole length or its distance to borehole increases.
- For the cooling-dominated condition like the Bioscience node, the average ground temperature increase would decrease the cooling COP and further increase the load for the chillers. Based on the COP variation analysis, it is found that both load amplitude changes and load imbalance

conditions would cause an apparent increase in the electricity consumption per unit load. Hence, it is important to design the control loop to avoid these two conditions.

Based on the findings from this study, the following work would be conducted in the future.

- More detailed soil properties and ground topography would be measured, and a more detailed ground model would be built using Leapfrog Software.
- The 5GDHC network design plans would be determined. This includes the design of building-sited energy transfer station (ETS) with electrical heat pump and associated thermal energy storage. The control strategy would be investigated.
- The topology and characteristics of the piping for the 5GDHC network would be determined based on the Bioscience node location and the functions of the network.
- The model of 5GDHC network coupled with primary GSHP design would be implemented using the Modelica Buildings Library.
- The role of GSHP in the whole system would be restudied and redesigned for the new load distribution.

Acknowledgments

This material was based upon work supported by the U.S. Department of Energy, Office of Energy Efficiency and Renewable Energy (EERE), Office of Technology Development, Geothermal Technologies Office, under Award Number DE-AC02-05CH11231 with LBNL, and the National Science Foundation, Award Number #1903296 "CMMI-EPSRC: Modeling and Monitoring of Urban Underground Climate Change (MUC2)", to Prof. Kenichi Soga. We thank the following individuals. Sally McGarrahan and Kira Stoll of UC Berkeley provided overall guidance on energy use and infrastructure for the UC Berkeley campus and their teams provided data. Erica Levine of Arup for shared her insights on the Arup study. Charlie Carasis (UCB) provided the GIS data shown in Fig. 10. Dr. Xiang Sun (formerly UCB) gave useful suggestions to conduct the dealii simulations presented in Section 5. Dr. Tim Kneafsey (LBNL) provided access to his facilities to measure rock thermal conductivity values on core samples, whereas Dr. Shenghan Zhang (UCB) made the measurements. The borehole data visualization for this paper was generated using Leapfrog Software. Copyright © Seequent Limited. Leapfrog and all other Seequent Limited product or service names are registered trademarks or trademarks of Seequent Limited.

REFERENCES

American Society of Heating, Refrigerating and Air-Conditioning Engineers. "2015 ASHRAE Handbook—HVAC Applications (SI)". Atlanta, GA: American Society of Heating, Refrigerating and Air Conditioning Engineers, 2015.

Arndt, D., Bangerth, W., Blais, B., Clevenger, T.C., Fehling, M., Grayver, A.V., Heister, T., Heltai, L., Kronbichler, M., Maier, M., Munch, P., Pelteret, J.-P., Rastak, R., Thomas, I., Turcksin, B., Wang, Z., Wells, D., "The deal.II Library, Version 9.2", Journal of Numerical Mathematics, vol. 28, pp. 131-146, 2020.

Arup North America Ltd, "UC Berkeley Energy Delivery Options Final Report", Arup, 2015.

Buffa, S., Cozzini, M., D'Antoni, M., Baratieri, M., & Fedrizzi, R. "5th generation district heating and cooling systems: A review of existing cases in Europe.", Sustainable Energy Reviews, vol. 104, pp. 504-522, 2019.

Geuzaine, C., & Remacle, J.-F., "Gmsh: a three-dimensional finite element mesh generator with built-in pre- and post-processing facilities", International Journal for Numerical Methods in Engineering, vol. 79, no. 11, pp. 1309-1331, 2009.

Kavanaugh, S., & Rafferty, K., "Geothermal Heating and Cooling: Design of Ground-Source Heat Pump Systems", ASHRAE, 2014.

Li, R., Ooka, R., & Shukuya, M. "Theoretical analysis on ground source heat pump and air source heat pump systems by the concepts of cool and warm exergy.", Energy and Buildings, vol. 75, pp. 447-455, 2014.

Marion W, Urban K, "User's manual for TMY2's: Derived from the 1961-1990 national solar radiation data base.", Nasa Sti/recon Technical Report N, vol. 96, pp. 11274, 1995.

Phelps, G.A., Graymer, R.W., Jachens, R.C., Ponce, D.A., Simpson, R.W., & Wentworth, C.M., "Three-Dimensional Geologic Map of the Hayward Fault Zone, San Francisco Bay Region, California", USGS Scientific Investigations Map 3045: https://pubs.usgs.gov/sim/3045/, 2008.

Qian, H., & Wang, Y., "Application Analysis of Ground Source Heat Pumps in Building Space Conditioning", LBNL, 2013.

Staffell, I., Brett, D., Brandon, N., Hawkes, A., "A review of domestic heat pumps.", Energy & Environmental Science, vol. 5, no. 11, pp. 9291-306, 2012.

Sulzer, M., Werner, S., Mennel, S., & Wetter, M., "Vocabulary for the fourth generation of district heating and cooling. Smart Energy", Smart Energy, vol. 1, pp. 100003, 2021.

Sun, X., Soga, K., Cinar, A., Su, Z., Chen, K., Kumar, K., Dobson, P.F., & Nico, P.S., "An HPC-Based Hydrothermal Finite Element Simulator for Modeling Underground Response to Community-Scale Geothermal Energy Production", Proceedings: Forty Sixth Workshop on Geothermal Reservoir Engineering, Stanford University, 2021.